Nuclear Safety
2021

Benchmark Study of the Accident at the Fukushima Daiichi Nuclear Power Plant

Summary Report

OECD
BETTER POLICIES FOR BETTER LIVES

NEA
NUCLEAR ENERGY AGENCY

Nuclear Safety

Benchmark Study of the Accident at the Fukushima Daiichi Nuclear Power Plant

Summary Report

NEA No. 7525

NUCLEAR ENERGY AGENCY
ORGANISATION FOR ECONOMIC CO-OPERATION AND DEVELOPMENT

ORGANISATION FOR ECONOMIC CO-OPERATION AND DEVELOPMENT

The OECD is a unique forum where the governments of 38 democracies work together to address the economic, social and environmental challenges of globalisation. The OECD is also at the forefront of efforts to understand and to help governments respond to new developments and concerns, such as corporate governance, the information economy and the challenges of an ageing population. The Organisation provides a setting where governments can compare policy experiences, seek answers to common problems, identify good practice and work to co-ordinate domestic and international policies.

The OECD member countries are: Australia, Austria, Belgium, Canada, Chile, Colombia, Costa Rica, the Czech Republic, Denmark, Estonia, Finland, France, Germany, Greece, Hungary, Iceland, Ireland, Israel, Italy, Japan, Korea, Latvia, Lithuania, Luxembourg, Mexico, the Netherlands, New Zealand, Norway, Poland, Portugal, the Slovak Republic, Slovenia, Spain, Sweden, Switzerland, Turkey, the United Kingdom and the United States. The European Commission takes part in the work of the OECD.

OECD Publishing disseminates widely the results of the Organisation's statistics gathering and research on economic, social and environmental issues, as well as the conventions, guidelines and standards agreed by its members.

NUCLEAR ENERGY AGENCY

The OECD Nuclear Energy Agency (NEA) was established on 1 February 1958. Current NEA membership consists of 34 countries: Argentina, Australia, Austria, Belgium, Bulgaria, Canada, the Czech Republic, Denmark, Finland, France, Germany, Greece, Hungary, Iceland, Ireland, Italy, Japan, Korea, Luxembourg, Mexico, the Netherlands, Norway, Poland, Portugal, Romania, Russia, the Slovak Republic, Slovenia, Spain, Sweden, Switzerland, Turkey, the United Kingdom and the United States. The European Commission and the International Atomic Energy Agency also take part in the work of the Agency.

The mission of the NEA is:

– to assist its member countries in maintaining and further developing, through international co-operation, the scientific, technological and legal bases required for a safe, environmentally sound and economical use of nuclear energy for peaceful purposes;

– to provide authoritative assessments and to forge common understandings on key issues as input to government decisions on nuclear energy policy and to broader OECD analyses in areas such as energy and the sustainable development of low-carbon economies.

Specific areas of competence of the NEA include the safety and regulation of nuclear activities, radioactive waste management and decommissioning, radiological protection, nuclear science, economic and technical analyses of the nuclear fuel cycle, nuclear law and liability, and public information. The NEA Data Bank provides nuclear data and computer program services for participating countries.

Cover photos: Fukushima Daiichi Nuclear Power Plant (Creative Commons; Dean Calma/IAEA).

Acknowledgements

The following representatives from the participating organisations are acknowledged for their contributions to the project and to the authoring of this report.

Operating agent:

Institute of Applied Energy (IAE-Japan)

Participating organisations and authors:

IAE (Japan): M. Pellegrini

CSN/CIEMAT (Spain): L.E. Herranz, C. López

GRS (Germany): M. Sonnenkalb, M. Sogalla

PSI (Switzerland): T. Lind, L. Fernandez Moguel

JAEA (Japan): Y. Maruyama

NRA(S/NRA/R) (Japan): H. Hoshi

CRIEPI (Japan): Y. Nishi

IRSN (France): D. Jacquemain

IBRAE (Russian Federation): K. Dolganov

KAERI (Korea): J.H. Song, S.I. Kim, T.W. Kim

CEA (France): C. Journeau, G. Ducros, Y. Pontillion, L. Godin-Jacqmin

NRC/DOE/EPRI (United States): N. Andrews (SNL), R. Lee (NRC), D. Peko (DOE), R. Wachowiak (EPRI)

CNL (Canada): A. Morreale

VTT (Finland): T. Sevon

Table of contents

List of figures

List of tables

List of abbreviations and acronyms

ADS	Automatic depressurisation system
ATD	Atmospheric transport and dispersion
AWI	Alternative water injection
BSAF	Benchmark Study of the Accident at the Fukushima Daiichi Nuclear Power Station
BWR	Boiling water reactor
CAMS	Containment air measurement system
CEA	Alternative Energies and Atomic Energy Commission (France)
CNL	Canadian Nuclear Laboratories
CRIEPI	Central Research Institute of Electric Power Industry (Japan)
Cs	Cesium
CIEMAT	Research Centre for Energy, Environment and Technology (Spain)
DOE	Department of Energy (United States)
D/W	Dry well
FP	Fission product
GRS	Gesellschaft für Anlagen- und Reaktorsicherheit (Global Research for Safety)
HPCI	High pressure coolant injection
I	Iodine
IAE	Institute of Applied Energy (Japan)
IBRAE	Nuclear Safety Institute of the Russian Academy of Sciences
IRSN	Radioprotection and Nuclear Safety Institute (France)
JAEA	Japan Atomic Energy Agency
KAERI	Korea Atomic Energy Research Institute
MCCI	Molten core concrete interaction
MP	Monitoring post
MSL	Main steam line
NEA	Nuclear Energy Agency
NG	Noble gas
NRA(S/NRA/R)	Regulatory Standard and Development Department Secretariat of the Nuclear Regulatory Authority (Japan)
NRC	Nuclear Regulatory Commission (United States)
PCV	Primary containment vessel
PSI	Paul Scherrer Institute (Switzerland)

PWR	Pressurised water reactor
RCIC	Reactor core isolation cooling
RCS	Reactor cooling system
RPV	Reactor pressure vessel
SA	Severe accident
SAMGs	Severe accident management and guidelines
S/C	Suppression chamber (torus)
SRV	Safety relief valve
ST	Source term
SNL	Sandia National Laboratories (United States)
TEPCO	Tokyo Electric Power Company (Japan)
VTT	Technical Research Centre of Finland
WSPEEDI	Worldwide version of System for Prediction of Environmental Emergency Dose Information
Xe	Xeron

Executive summary

The Great East Japan earthquake occurred on 11 March 2011 at 2:46 p.m. JST (Japan Standard Time). At the onset of the earthquake, the operating units at the Tokyo Electric Power Company's (TEPCO) Fukushima Daiichi Nuclear Power Plant were automatically shut down. However, the subsequent tsunami and flooding of critical site areas and equipment produced conditions that were significantly beyond the design basis of the Fukushima Daiichi Nuclear Power Plant, resulting in three core meltdown accidents to the operating reactors.

In the aftermath of the event, the Japanese Ministry of Economy, Trade and Industry's Agency of Natural Resource and Energy proposed an international programme to the OECD Nuclear Energy Agency (NEA) to apply severe accident analysis codes to the simulation of the Fukushima Daiichi events. This initiative became the Benchmark Study of the Accident at the Fukushima Daiichi Nuclear Power Station (BSAF). Phase I of the project was initiated in 2012 and focused on the severe accident progression for the first six days. Phase II was established in April 2015 and extended the analysis to 21 days (500 hours) after the accident, including an analysis of fission product (FP) behaviour. Two generic objectives were defined:

- to provide information and analysis on the severe accident (SA) progression, FP behaviour and source term (ST) estimation, and to support safe and timely decommissioning of the Fukushima Daiichi Nuclear Power Plant;
- to contribute to the improvement of methods and models of the SA codes in order to reduce uncertainties in SA analysis.

Fourteen partners from eleven countries joined the project. A number of well-known SA codes have been applied, such as ASTEC, MAAP, MELCOR, SAMPSON, SOCRAT and THALES. Phase II of the project gave the participating organisations a chance to revise or consolidate their interpretation of the accident progression in units 1-3 from Phase I of the project.

The accident progression and associated code predictions for each of the three units are summarised below. Some conclusions and the main outcomes from the BSAF project are also included below. The accident transients are characterised by a paucity of data on the actual progression and a range of operator actions, with varying degrees of success in the face of the enormous challenges posed by the lack of power and reliable information.

During the unit 1 accident: For the first ten hours, the operators were largely blind as to the state of the reactor, but in time initiated measures to inject water into the reactor pressure vessel (RPV) to try to avoid or mitigate any fuel damage that might initiate from loss of coolant after so many hours with no water injection. They were, for the most part, not successful in their interventions. Attempts to inject emergency cooling water into the core were not successful, with considerable ambiguity about pipe routing within the primary containment vessel (PCV). Operators were not able to control the RPV pressure, and for the first 24 hours, they also could not control the PCV pressure. As a result, core damage is believed to have commenced early in the accident, 5-12 hours from shutdown. Unit 1 was the first reactor to have suffered severe damage. In this first 5-12-hour period, a yet to be identified failure or leak of the pressure boundary depressurised the RPV. As it was not possible to remove the decay heat or inject cooling water, the PCV pressure increased to the point that steam, hydrogen and fission products leaked to the environment, believed to have occurred in the PCV head flange region. In the BSAF project analyses, these key events were modelled using various assumptions of either leakage at the reactor cooling system (RCS) pressure boundary or a larger failure such as a main steam line (MSL) creep rupture or lower head attack by debris. All calculations predict pressure signatures generally consistent with the sparse RCS and PCV data points in this period.

All analyses predicted almost complete core melt and relocation, debris attack of the lower head (between about 7 and 15 hours), and near complete debris release to the pedestal region. Molten corium concrete interaction (MCCI) is predicted in all of the calculations, contributing to the high containment pressure until the suppression chamber (S/C) was manually vented at around 24 hours. After the vent, the PCV pressure was predicted generally to increase due to MCCI gas generation until a leakage in the containment is assumed in all calculations to match the observed drop in pressure. At around 270 hours, most of the calculations assumed an increase in the rate of alternative water injection (taken to be 0 prior to this time) and predicted an increase of the PCV pressure consistent with recorded data. This suggests that the ex-vessel core debris was still hot and the MCCI might have been ongoing. In fact, most calculations indicate that interaction of the molten material with concrete was still ongoing at 500 hours. It is important to note that there is no evidence as of yet from the unit 1 plant measurements, or subsequent in-containment investigations, to confirm this code prediction.

The release of fission products (noble gases [NG], cesium [Cs] and iodine [I]) is strongly linked to the onset of core degradation. Most calculations show a very rapid release of these FPs, with the total release from damaged fuel to the RPV and PCV reaching a limit generally above 80% of the initial inventory. Note that this predicted behaviour is common to all the units. The simulated containment FP distribution was influenced by the nature of the assumed RPV leak or failure, which affects the amount of FPs discharged into and scrubbed by the suppression pool. For most calculations, large amounts of Cs and I were scrubbed by the suppression pool during the early injection through the safety relief valves (SRVs), and a large amount of Cs was computed to be deposited on the upper structures of the RPV. Almost all calculations estimated a first FP release to the environment at around ten hours, when the PCV head flange is predicted to have commenced leaking. Each code’s ST prediction was compared against estimates from an inverse analysis of atmospheric releases derived using atmospheric transport and dispersion (ATD) codes/methods, such as the WSPEEDI code (Worldwide version of System for Prediction of Environmental Emergency Dose Information) and a GRS method. This comparison shows that the integral release after the PCV venting at around 24 hours was fairly well predicted across all code calculations, with a variability of about 1 order of magnitude relative to the estimation.

The unit 2 accident was characterised by the operation of the reactor core isolation cooling (RCIC) system for around 70 hours in an unanticipated “self-regulating” mode. The mechanism is not yet fully understood, but it is believed that the uncontrolled full flow RCIC injection overfilled the RPV up to the steam lines, driving two-phase steam and water into the RCIC turbine. The rise in the PCV pressure during this period of RCIC operation is lower than expected, and believed to be the result of stratification of the suppression pool and additional heat removal due to partial flooding of the torus room by seawater during the tsunami. After around 70 hours, the RCIC system failed, prompting operators to depressurise the RPV and attempt low-pressure injection using fire trucks. This action was unsuccessful, and the water level in the RPV decreased, leading to core damage.

All participants reasonably captured the main trends observed in the plant measurements (i.e. the high RPV pressure and water level and the gradual pressurisation of the PCV) during the RCIC operation period. The simulated core heat up and degradation phase started at about 75 hours, shortly after operators depressurised the RPV. This phase was characterised by three large pressure transients in the RPV and the PCV. These transients are calculated to arise from hydrogen released by oxidation of core materials that experienced renewed access to steam while slumping into the lower plenum. Generally, participants that predicted a greater mass of hydrogen production (in excess of 800 kg) were able to predict a PCV pressure transient that was in closer agreement with the measurements. Most calculations predict lower-head failure between 83 and 129 hours and consequent release of 16-161 tonnes of debris into the pedestal. Here, the analyses predicted ongoing transfer of mass from the failed vessel to the reactor cavity and had difficulty predicting the significant materials remaining in the lower head that is suggested by the TEPCO muon tomography examinations. Most of the calculations did not predict the onset of MCCI at unit 2. For those that did, the degree of MCCI as well as the extent of predicted radial and axial erosion of the reactor pedestal depended strongly on other modelling assumptions.

In unit 2, no leaks were predicted or assumed to connect the RPV to the dry well (D/W) across all code calculations prior to RPV failure. Thus, volatile FPs released through core degradation were transferred to the S/C through the operating SRV and further to the D/W through the operating vacuum breakers. Evaluation of the code calculations against the measured S/C dose rate data from the continuous air measurement systems (CAMS) showed reasonable agreement with the timing of increases or decreases in the dose rate. While the majority of code calculations tended to over-predict the measured dose rate by a factor of 3-4, the agreement is remarkable nonetheless. A few participants were able to predict the measured D/W dose rate increase at the postulated time of lower head failure around 95 hours. Estimation by the ST inverse analyses showed a first peak release of FPs to the environment at about the time of the first RPV pressure peak, followed by additional peak releases some hours later. A few participants predicted such a first peak release, though the magnitude of the predicted release was considerably lower than the release estimates based on environmental measurements because the PCV pressure was not large enough to justify a PCV leak in the calculations. Almost all calculations predicted a large release of FPs to the environment later, at the time of the PCV failure (about 89 hours), which entered the environment through the open reactor building blowout panel by various presumed leakage paths from the PCV. The variation in the code calculations of the total FP release to the environment was within one order of magnitude of the estimates by the backwards calculations.

The unit 3 accident was characterised by the normal functioning of heat removal from the RPV in the first 35 hours of the accident, first by the RCIC system, then by the high pressure coolant injection (HPCI) system. While these systems performed normally, their operation replaced water lost from the RPV and moved heat from the reactor fuel to the suppression pool and the PCV atmosphere. The increase in PCV pressure due to steady injection of steam was controlled in a later phase of the accident by activation of sprays in the S/C.

During this first accident period, all of the participants predicted the main signatures in the RPV and PCV reasonably well. After the HPCI was stopped, unit 3 experienced a period of about ten hours with no coolant injection into the reactor, which is thought to have caused the water level to drop below the bottom of the fuel. Most of the analyses show that core degradation starts during this time, and was accompanied by hydrogen generation, causing further pressurisation of the PCV. The reactor is postulated to have depressurised by spurious operation of the automatic depressurisation system (ADS), from about 42 hours, until the hydrogen explosion in the unit 3 reactor building, at 68 hours. This period was characterised by a number of attempts by operators to depressurise the containment and inject water into the RPV using fire trucks. As shown by most of the analyses, core degradation was characterised by a number of core slumping events, leading to a number of periods of D/W pressure increase mitigated by either containment venting or leakage out of an impaired D/W upper head. Progressive core damage was predicted by all calculations to ultimately result in a failure of the RPV lower head between about 43 hours and 73 hours. Due to the large debris discharge in the containment, the MCCI was predicted by most codes, and persisted in the analyses until 500 hours (the end of the simulation). Even though large amounts of debris in the reactor pedestal were observed by direct inspection (heights up to 2.5 metres), the occurrence of the MCCI for such a long period of time has not been confirmed by post-accident investigations.

Comparison of FP data against D/W CAMS dose rate measurements determined that calculations which assume a moderate leakage from the RPV to the D/W before RPV failure predict a dose rate increase in closer agreement to the onsite and offsite ground and air measurements. Across all the calculations, large fractions of Cs and I were predicted to be retained in the suppression pool water and large fractions of Cs were predicted to deposit on the RPV wall. The main FP release to the atmosphere from unit 3 was calculated to take place from 45 hours to 70 hours during the first two containment vents and at the time of the hydrogen explosion. Comparisons with the ST inverse analyses show that most calculations predicted releases to the atmosphere of the same order of magnitude as the backwards estimates, with releases of less than 0.5% of Cs and less than 2% of I.

In conclusion, from the point of view of the accident progression, the BSAF project has helped to clarify a large number of uncertainties that were initially identified regarding the operation of safety systems, alternative water injection, the period of core degradation and relocation, and the main distribution of debris and FPs within the units. Despite the many clarifications, there remain several areas specific to the Fukushima accident transients that are worthy of further investigation, including refinement of core degradation periods, hydrogen generation, MCCI progression, correlation of CAMS response and details of the source terms, especially the FP transport by water leakages from the PCV. In addition, key issues identified through this study are the debris transported through the core plate, lower head failure mode and debris discharge into containment, debris retention by structures below the RPV such as control rod drives and instrumentation tubes, long-term MCCI progression and containment failure modes. By continued post-accident investigations during the decommissioning of the Fukushima Daiichi reactors, valuable information could be provided to close some of these issues. In fact, recent plant inspections (i.e. muon tomography and PCV internal assessment) have already provided observations that present challenges for the current code modelling. In addition, the analyses of the BSAF have highlighted many uncertainties in the accident boundary conditions, such as the amount and timing of alternative water injection, systems' leak paths and component off-nominal behaviour might affect the results of the analyses regardless of how accurate the in-code models are. Fission product modelling has also brought up issues that need further improvement in the present codes: pool scrubbing under high temperature and high gas velocities; iodine chemistry, FP transport by water leakages from the RPV and the PCV, remobilisation of FPs in the long run and under the effect of some accident management procedures, etc.

Looking beyond these specific conclusions, the BSAF activities have had a significant impact on the diverse and numerous stakeholders in the nuclear power community. These stakeholders include the large group of researchers that has directly participated in the BSAF programme, as well as governmental and regulatory organisations around the world, TEPCO and industry partners, and the general public.

Perhaps one of the most fundamental contributions of the BSAF project has been to improve the understanding of the accident sequences. Through the diversity of the modelling codes and approaches, and the use of parametric studies, it has been possible to identify the more likely scenarios that can fit with the limited data. As more information becomes available through decommissioning, these scenarios can be further down-selected and refined.

This significant understanding of the progression of the accidents among the technical participants has both clarified to analysts the essential details of the accident progression and provided deep insights into future code and model improvements to advance predictive capabilities (as described above). The BSAF analyses have served to address many uncertainties that underlie current regulatory practices with respect to source term characteristics and major assumptions such as the timing, magnitude and duration of severe accident radiological releases, as well as pointing to improvements in regulatory oversight and protective measures in emergency response to severe accidents. The industry has used the BSAF analytical findings to improve accident management procedures, water management and containment protection. Additionally, a major outcome of the BSAF programme and the resulting improved severe accident code performance has been to provide information useful to the decades-long decommissioning activities and to help inform decommissioning technologies with respect to likely distributions of core materials and their likely morphology and material composition for optimal design of tools and extraction approaches. Finally, the public benefits from the understanding of nuclear accidents and their consequences and the demonstrated competence in explaining what happened at Fukushima. With the existential threats posed by climate change and global warming, it is ever more critical that the nuclear industry demonstrates understanding and competency in the use of nuclear technology as a source of low-carbon energy. Programmes such as the BSAF can help dispel unwarranted fear and increase understanding of nuclear technology.

Chapter 1. Introduction

The Tokyo Electric Power Company (TEPCO) shut down its units at the Fukushima Daiichi Nuclear Power Plant when the Great East Japan earthquake occurred on 11 March 2011 at 2:46 p.m. JST (Japan Standard Time). At first, safety systems were operated successfully to remove decay heat, driven by diesel generators. However, the subsequent tsunami flooded critical on-site power systems and resulted in the extended loss of the ultimate heat sink. This produced beyond design-basis conditions in units 1, 2 and 3 and ultimately led to core meltdown in the three units.

Since 2011, TEPCO has successfully implemented efforts at the plant to visualise and quantify the conditions of the reactors through external (i.e. muon tomography) and internal inspections (i.e. primary containment vessel [PCV] entry). The results of the muon investigation show that in all reactors, little fuel remains in the core region, confirming the idea of large core meltdown occurring in all the reactors due to the total or partial loss of core cooling. In addition, the PCV inspection showed that some degree of debris discharge ex-vessel was experienced in all of the units.

After the accident, in December 2011, the Japanese government and TEPCO compiled the "Roadmap towards Restoration from the Accident at Fukushima Daiichi Nuclear Power Station". The roadmap was revised in June 2013 to accelerate the schedule for removing fuel debris and other restoration measures. As per the roadmap, the Japanese Ministry of Economy, Trade and Industry's Agency of Natural Resource and Energy has been promoting the Research and Development Plan towards the Decommissioning of the Fukushima Daiichi Nuclear Power Plant units 1-4, which includes an analysis of the accident progression at units 1-3 and their current status.

In a number of the Nuclear Energy Agency (NEA) member countries, severe accident (SA) analysis codes had been developed after the accident at the Three Mile Island unit 2 reactor. These computer codes were also used to analyse the accident at the Fukushima Daiichi Nuclear Power Plant, and valuable information and estimations were provided regarding the accident progression.

Taking these circumstances into account, with the participation of some NEA countries, working plans were set up to conduct a benchmark study of the accident progression of units 1-3 during the Fukushima Daiichi Nuclear Power Plant accident using computer codes and methods of analysis. This culminated in the "Benchmark Study of the Accident at the Fukushima Daiichi Nuclear Power Station" (BSAF), an international programme proposed by the aforementioned Agency of Natural Resource and Energy. The NEA Committee on the Safety of Nuclear Installations decided to support the BSAF. After discussion among the related countries and organisations, the BSAF project was launched in November 2012. The project included participants from 21 organisations in 11 countries.

Many years will be required to completely reveal the status of the units, including quantitative debris distribution, and the accident progression that occurred in each of the three units. Thus, a phased approach has been applied, with two generic objectives. The first objective was to provide information and analysis on the SA progression, fission product (FP) behaviour and source term (ST) release estimation of the Fukushima Daiichi accident, including a comparison to measured plant data, to support safe and timely decommissioning of the Fukushima Daiichi Nuclear Power Plant. The second objective was to contribute to the improvement of methods and models of the SA codes applied by each participating organisation in order to reduce uncertainties in SA analysis and to validate SA analysis codes using data measured through the decommissioning process.

The BSAF project was conducted in two phases. Phase I began in November 2012 and ran until December 2014. It focused mainly on the phenomena of the core degradation and debris relocation inside the reactor pressure vessels and the PCVs of units 1-3 during the first six days. The project provided valuable insight on the accident progression and improved understanding of severe accident phenomena that took place during the accident in order to provide information on the current status of the units. Nonetheless, Phase I signatories recognised that, despite the key insights gained into the understanding of accident scenarios, another benchmark study was needed. Several reasons supported this initiative. Among them was the need to strengthen some of the insights into the accident so that a better understanding could be gained, and a desire to extend the time domain of the analysis to three weeks so that the analyses would encompass the stable and continuous cooling periods in all units, and to capture all potential melt relocations and main ST releases. This further required the inclusion of the reactor building as an essential building in the accident progression and the many dose rate measurements that have been recorded therein. Finally, a detailed review of FP release, transport and emission to the environment during the Fukushima Daiichi accident was included in Phase II of the study.

In line with this reasoning, a second phase of the project was proposed to build upon the success of the first phase, with the following major objectives:

- provide information and analysis on the SA progression, FP behaviour, ST estimation and comparison with measured plant data within the first three weeks of the Fukushima Daiichi accident (units 1-3) to support a safe and timely decommissioning;
- improve the methods and models of the computer codes aimed at reducing uncertainties in SA analysis

Phase II began in April 2015 and was finished in March 2018, providing the participating organisations with a chance to revise or consolidate their interpretation of the accident progression in each unit, to continue the comparison with the additional measurement data that became available later in the accident, and to compare the predicted FP releases with direct measurements or estimations generated by environmental dispersion codes. Additionally, the latest information obtained by TEPCO investigations at the plant provided more details on the current condition of the units, which provided guidance to the participating organisations in the estimation of the accident scenario.

Table 1.1 provides a list of the countries and organisations that participated in Phase II, as well as the analysis performed and the code(s) used.

This report summarises the progress made in Phase II. It begins with a discussion of the severe accident codes, with an emphasis on the differences and similarities among the approaches used by the participants. It then summarises the results of the ST estimations based on measured plant data and the atmospheric FP transport and dispersion results based on the STs calculated. Finally, it provides some conclusions and a synthesis of the lessons learnt, as well as recommendations for potential forthcoming studies of the accidents.

Table 1.1. **Participants, employed codes and analytical work in Phase II of the BSAF project**

	Country	Partner	Code	Analytical work
1	Canada	Canadian Nuclear Laboratories (CNL)	MELCOR	Unit 2
2	Finland	Technical Research Centre of Finland (VTT)	MELCOR2.2	Units 1-2-3
3	France	Alternative Energies and Atomic Energy Commission (CEA)	TOLBIAC	Unit 1 (MCCI)
4	France	Radioprotection and Nuclear Safety Institute (IRSN)	ASTEC V2.0 rev3 p1	Units 1-2-3
5	Germany	GRS	GRS Code	Inverse analysis
6	Japan	Central Research Institute of Electric Power Industry (CRIEPI)	MAAP 5.01	Unit 3
7	Japan	Japan Atomic Energy Agency (JAEA)	THALES 2	Units 1-2-3
8	Japan	Institute of Applied Energy (IAE)	SAMPSON-B 1.4 beta	Units 1-2-3
9	Japan	Nuclear Regulation Authority NRA(S/NRA/R)	MELCOR 2.1	Units 1-2-3
10	Korea	Korea Atomic Energy Research Institute (KAERI)	MELCOR 1.8.6	Unit 1
			MELCOR 2.1	Unit 2
11	Russia	Nuclear Safety Institute of the Russian Academy of Sciences (IBRAE)/Rosatom	SOCRAT/V3	Unit 1
12	Spain	Nuclear Security Council (CSN)/Research Centre for Energy, Environment and Technology (CIEMAT)	MELCOR 2.1-4803	Unit 1
13	Switzerland	Paul Scherrer Institute (PSI)	MELCOR 2.1_4203	Unit 3
14	United States	Nuclear Regulatory Commission (NRC)/Department of Energy (DOE)/Sandia National Laboratories (SNL)	MELCOR 2.1-5864	Units 1-2-3
			HYSPLIT	Forward analysis

Chapter 2. Results of the unit 1 analyses

Overview of the unit 1 accident

As summarised earlier, the unit 1 accident proceeded with essentially no effective intervention by the operators, unsuccessful attempts to inject emergency cooling water into the core, no operator control of the reactor pressure vessel (RPV) pressure, and for the first 24 hours, no active control of primary containment vessel (PCV) pressure. Because of this, core damage is calculated to have commenced early in the accident, between 5 and 12 hours from scram, and was the first reactor to have suffered severe damage. In this first 5-12-hour period, the RPV self-depressurised by some yet unidentified failure/leak of the pressure boundary. Because of the inability to reject decay heat or inject cooling water, the PCV pressure ultimately became very high, which is believed to have led to leakage of steam, hydrogen and fission products (FPs) to the environment in the PCV head flange region. In the project analyses, these key events were modelled using various assumptions of either leakage at the reactor coolant system (RCS) pressure boundary or a larger failure, such as a main steam line (MSL) creep rupture or lower head attack by debris. All calculations predict signatures generally consistent with the sparse RCS and PCV data points in this period. The following sections describe the key results from participants' analyses of each unit.

Thermal hydraulics and core degradation

The RCS pressure in unit 1 was only manually measured twice by operators between 5 and 12 hours. These measurements (Figure 2.1a) indicate that an RPV depressurisation event occurred sometime between 5 and 12 hours. The timing of the RCS leakage or RPV failure in the simulations varied, depending on the hypothesis made by the modellers (Table 2.1). Most leakages, though, were predicted to occur between three and four hours, regardless of the path chosen. The differences related to the leakage assumptions (boundary conditions in the codes) during the pressure vessel degradation are visible in the RPV pressure evolution.

Figure 2.1. **Comparison of analyses results versus measurements for unit 1: Reactor pressure vessel pressure and dry well pressure**

A. Reactor pressure vessel pressure

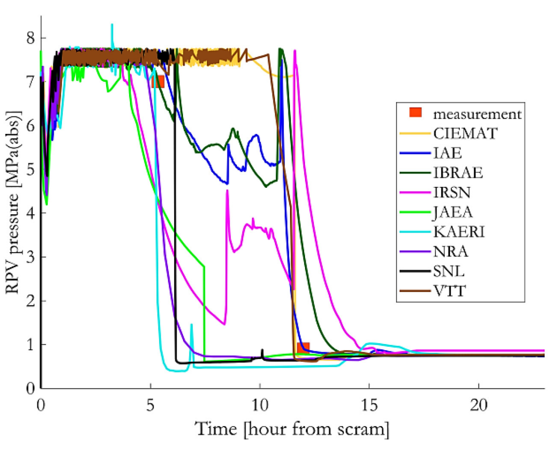

B. Dry well pressure

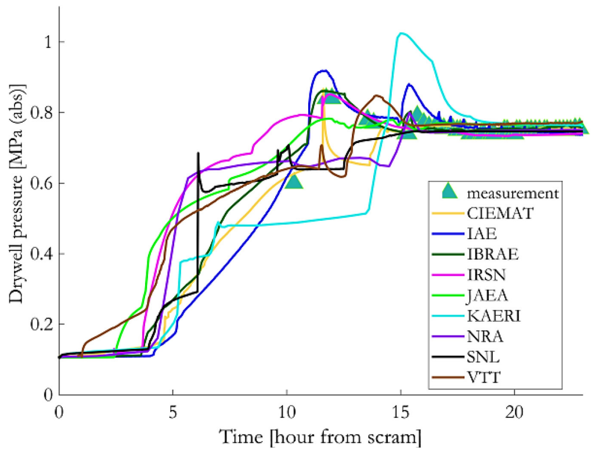

From Table 2.2, two modelling teams (Korea Atomic Energy Research Institute [KAERI] and Sandia National Laboratories [SNL]) modelled an MSL failure (at 5 hours and 6.1 hours respectively) based on high RPV pressures and high core exit gas temperatures, resulting in an immediate reactor depressurisation following the failure. All other teams assumed an RCS leak occurs at some penetration(s) (safety relief valve [SRV], source range monitor, transverse instrumentation probe or primary loop recirculation), producing a gradual loss of the RPV pressure. Some institutes (Research Centre for Energy, Environment and Technology [CIEMAT], Nuclear Safety Institute of the Russian Academy of Sciences [IBRAE] and the Nuclear Regulation Authority [NRA]) even assume two leakage pathways. Dry well (D/W) pressurisation is the result of water, steam and hydrogen (generated from zirconium-steam reactions during the core degradation) release from the RPV and the absence of any heat rejection from the PCV.

Table 2.1. **Unit 1 event time of reactor cooling system leak or failure**

In hours

	CIEMAT	IAE	IBRAE	IRSN	JAEA	KAERI	NRA	SNL	VTT
SRM/TIP pipe	1.0	–	3.6	–	2.47	–	4.1	–	–
SRV gasket	4.61	4.1	10.9	3.68	–	–	4.2	–	–
PLR pump leak	–	–	–	–	–	–	–	–	1.0
MSL failure	–	–	–	–	–	5.0	–	6.1	–

Note: SRM: source range monitor; TIP: transverse instrumentation probe; SRV: safety relief valve; PLR: primary loop recirculation; MSL: main steam line.

There is some variation in the prediction of the RPV failure time and mode between the calculations (Table 2.2). CIEMAT and the Technical Research Centre of Finland (VTT) predicted the lower head failure time by melt through or penetration failure respectively, coincident with the timing of the largest measured PCV pressure at around 11.5 hours. The Radioprotection and Nuclear Safety Institute (IRSN), the IBRAE and the Institute of Applied Energy (IAE) justified the PCV pressure increase with the assumption that the rise was generated by the slumping of debris in the lower head and predicted RPV failure a few hours later. The Japan Atomic Energy Agency (JAEA) predicted an earlier vessel failure and associates this pressure rise with the molten core concrete interaction (MCCI) progression. KAERI, the NRA and the SNL predicted the pressure rise either later or before the measured point at the onset of the MCCI phase.

Table 2.2. **Unit 1 event time of reactor pressure vessel failure and failure mode**

	CEA	CIEMAT	IAE	IBRAE	IRSN	JAEA	KAERI	NRA	SNL	VTT
Lower plenum failure (hours)	–	11.58	14.97	15.10	17.16	7.45	13.50	13.6	12.5	11.42
Failure mode	–	Melt through	Penetration failure	Melt through	Creep	Melt through	Penetration failure	Melt through	User specified	Penetration failure
Total masses in pedestal (tonnes)	39[1]	129	148	196	282[2]	130	136	115	154	111

1. This value includes only the debris mass in two sumps, since the CEA's calculation with TOLBIAC considers only the sumps. It does not consider the mass above the pedestal and dry well floor.

2. The IRSN value includes the mass of all in-core materials and the mass of the reactor pressure vessel lower head and is a modelling hypothesis.

Figure 2.2 shows the H_2 generation partially responsible for the PCV pressure increase during the first ten hours. As expected, the different predicted RPV depressurisation behaviours match the available PCV pressure data in different ways (Figure 2.1b). Those calculations that did not assume direct steam release into the D/W (KAERI and SNL) show a mild pressurisation until a peak at the time of the MSL break and, from then on, a subsequent pressure increase as long as some water remains in the RCS. Assuming the leakage in the RCS as a result of either the temperature increase (SRV, source range monitor) or from equipment leakage (primary loop recirculation pump) generally produced a slight depressurisation of the RPV and continuous containment pressurisation from steam discharging into the D/W. It should be also highlighted that the data predicted by most participants between 15 hours and the PCV venting time (around 24 hours) is consistent with the measurements. The relative steady state during this period is interpreted in most cases as a natural PCV pressure "self-regulation" balancing the pressure increase resulting from MCCI with PCV leakage through the flange of the upper head of the D/W into the reactor building. This is thought to be due to elastic stretching of the PCV head bolts under high strain from the PCV internal pressure.

Figure 2.2. **Unit 1 in-vessel hydrogen generation**

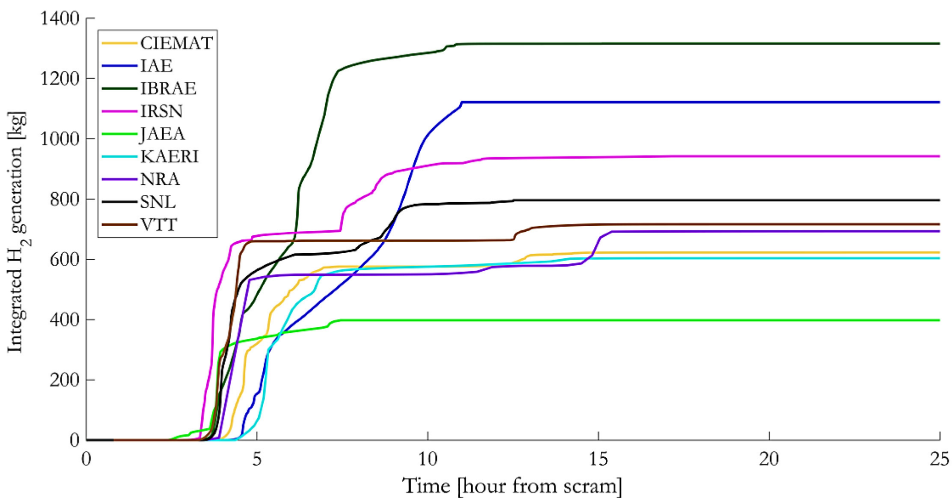

The majority of institutes modelled instantaneous corium spreading within the pedestal or in the sump (2.5-3 metres) as a default in the code, and evaluated the erosion from this point. Only the IAE calculated the process of corium spreading out the pedestal into the D/W. After the suppression chamber (S/C) vent closure (24.68 hours), the reactor building experienced a hydrogen explosion (24.83 hours) and the continuous gas release from the MCCI drove a pressure rise in the PCV until 50 hours, when the trend reversed and decreased for more than 200 hours until it sharply started increasing again at 270 hours from the reactor scram (Figure 2.3a).

All the calculations follow the measurements (Figure 2.3a) by assuming a containment leak of a variable cross-section from 50 hours on, with the exception of the JAEA, which instead postulated venting from the S/C. Among the institutes that assumed a containment leakage, three assumed that the leak occurred at a penetration, while the other five assumed that the leak was the result of MCCI erosion of the D/W liner, consistent with calculated MCCI erosion behaviour. This assumption is further supported by the Tokyo Electric Power Company (TEPCO) PCV investigations showing water leaking into the torus room, presumably from the sand cushion region outside of the PCV liner (TEPCO, 2013). Calculations rendered different decreasing slopes, depending on the gas mass flow rate imbalance between the MCCI and leaking flow rate.

At around 270 hours, a few calculations captured the changing trend by imposing an effective water injection (into the RPV and ultimately to the cavity floor); however, as shown in Figure 2.3b, they agree on an injection rate lower than 4.5 kg/s, but they differ on the specific injection profile.

At the time of the RPV lower head failure, most calculations predicted a total degraded core mass released in between 120 tonnes and 190 tonnes (Table 2.2), resulting in a massive amount of material at very high temperatures being relocated into the pedestal. In addition, despite no indication to confirm this based on plant inspections, almost all calculations predicted that interaction of the molten material with concrete was still ongoing at 500 hours (Figure 2.4).

Figure 2.3. **Unit 1: Primary containment vessel evolution over 0-500 hour period and alternative water injection mass flow rate**

A. Primary containment vessel evolution 0-500 hours

B. Alternative water injection mass flow rate

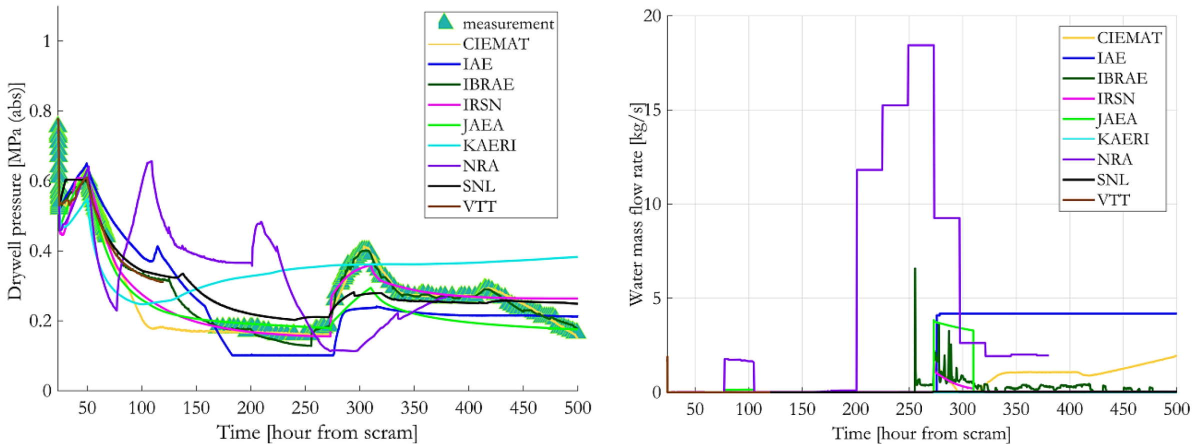

Figure 2.4. **Unit 1 concrete erosion depth (origin at the bottom of the sump)**

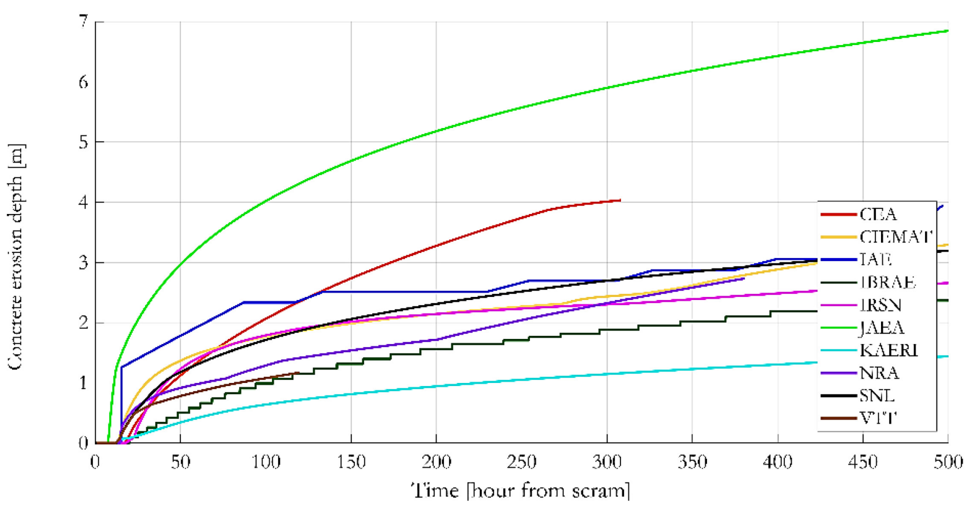

Fission product release and behaviour

Codes track the most relevant FPs, either as individual radionuclides or grouped into classes according to their chemical similarity. However, given the safety significance of cesium (Cs) and iodine (I) isotopes (Cs-137 and I-131, respectively) and the desire for a concise comparison, the analysis here is focused on these two elements. The initial inventory of every element for unit 1 was specified by the benchmark co-ordinator and in the case of Cs and I, they were 154.0 kg and

11.98 kg, respectively. The results hereafter are presented as an FP fraction based on the initial core inventory. Figure 2.5 shows the noble gas (NG) and I releases from the fuel in terms of fraction from the initial inventory. Given their volatile nature, NGs, Cs and I releases are strongly linked to core degradation. Most calculations predicted a fast release with or without subsequent steps according to core degradation progression up to getting an asymptotic value, which in most cases exceeded 80%.

The calculated results of the FP distribution in the containment were dependent on the assumptions made concerning the leaks from the RPV to the D/W, although in most cases radionuclides entered the PCV through the SRV discharge into the suppression pool. Most of the Cs and I was in aerosol form when it entered the PCV and once they were there, settled down from the atmosphere and deposited on D/W structures or were efficiently scrubbed after passing through the suppression pool. Typically, most analyses predicted less than 10% airborne concentrations, except in those cases that assumed a direct leakage from the RPV gas phase into the D/W. It is worth emphasising that significant deposition was predicted on the D/W structures and some remobilisation was noted in some calculations due to either PCV depressurisation or heating up of the structures beneath the deposits.

Figure 2.5. **Unit 1 mass fraction of fission products released from fuel**

A. Xeron (Xe)

B. Iodine (I)

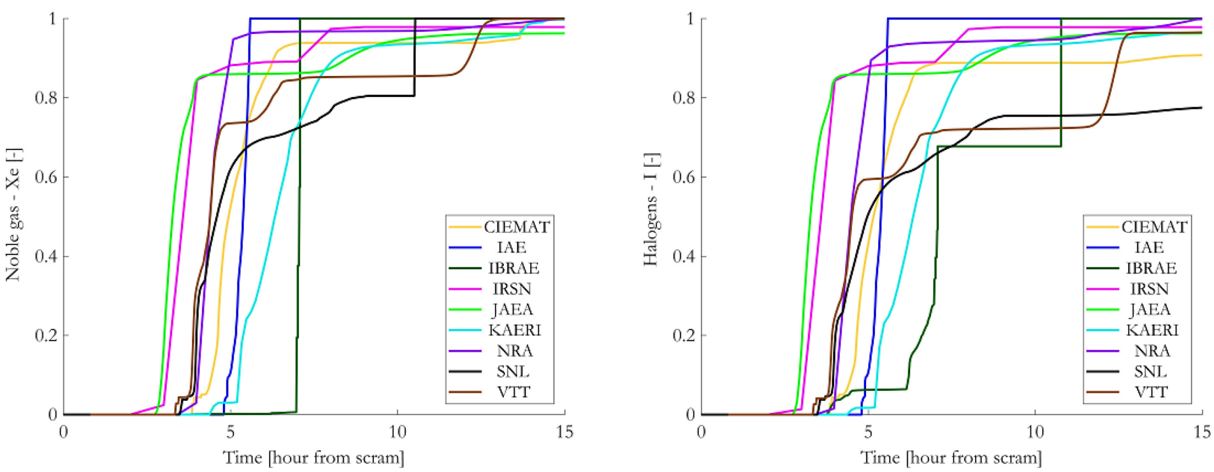

For most calculations, Cs and I were very efficiently scrubbed in the suppression pool during the early injection through the SRVs. At 35 hours, 10-80%, roughly, of Cs and I was estimated to have been scrubbed into the S/C water (Figure 2.6c and d). Differences in the calculations were due to the leak assumptions and the modelling of pool scrubbing geometry. Those calculations in which most FPs were injected through T-quenchers reached higher values of decontamination factor than those in which a good fraction of the FPs were transported into the pool through the down comers, which includes a non-condensable rich flow.

In the Fukushima Daiichi units, the dose rate in the D/W and the S/C of the PCV was measured by the containment air monitoring system (CAMS). Code results are only available for FP masses: airborne, deposited on structures, and dissolved or dispersed in water. For comparison with dose rates, a methodology of data conversion was developed by the operating agent (IAE) within the Phase II project, which relates FP masses to dose rates depending on their location and energy. In general, the conversion factor is larger for elements located either on the structures or for airborne ones and for FPs that have larger energy or, more precisely, a larger RHM value (Roentgen per hour per metre). The comparison accounts for decay and includes the effect of Xe-133, Cs-137, Cs-134 and I-131. Other elements, such as tellurium, are neglected in this conversion approach, but it is estimated that their consideration would have increased the estimated value by a factor of two. Details are provided in the final report.

Figure 2.6. **Unit 1 mass fraction of fission product deposited on structures in the dry well and solved in water in the suppression chamber**

Deposited on the structures in the dry well

A. Cesium (Cs) B. Iodine (I)

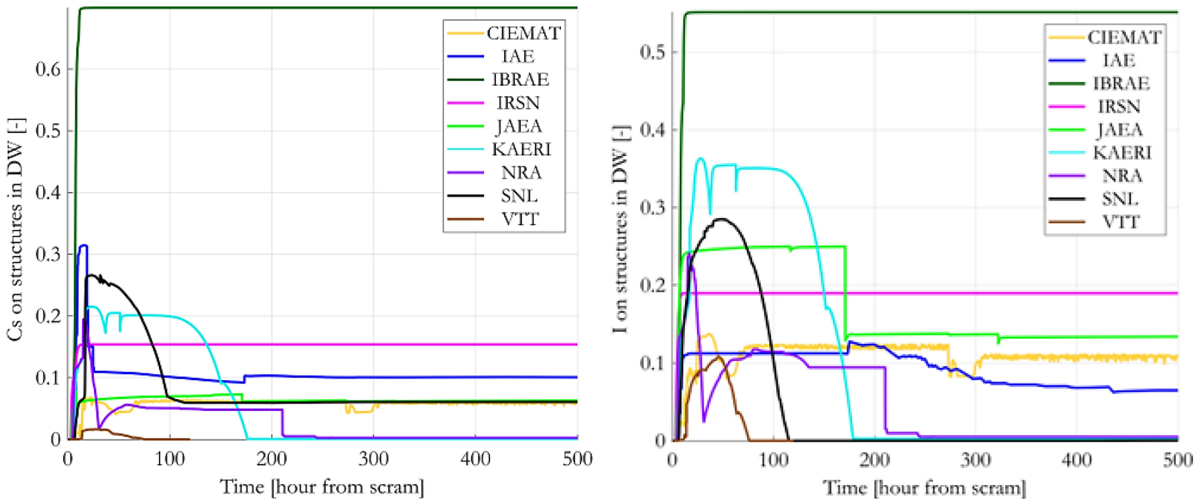

Solved in water in the suppression chamber

C. Cesium (Cs) D. Iodine (I)

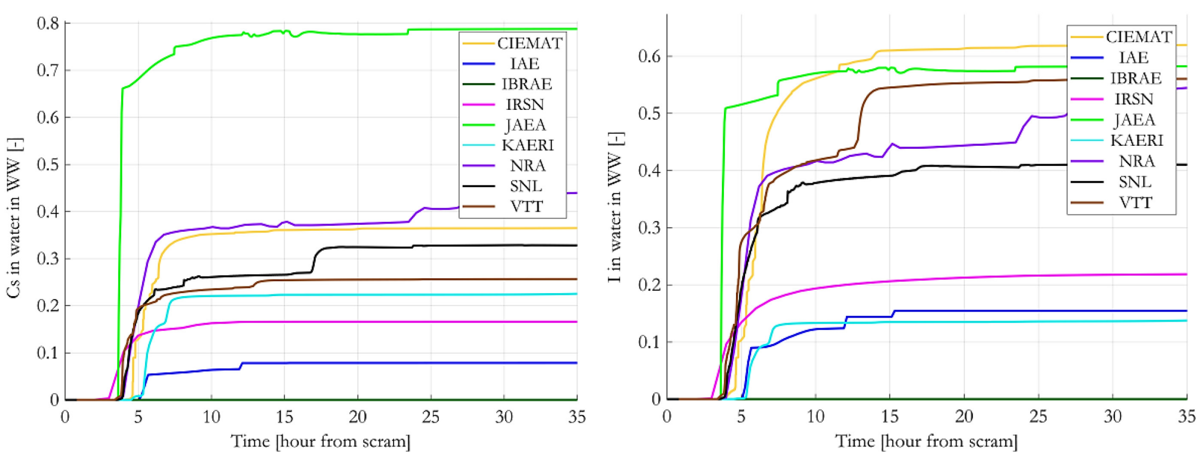

Figure 2.7 shows a comparison of the dose rate measurements by CAMS and the dose rates converted based on the analysis results. Both the measurements and analyses show large variations in the dose rate, but in general, the analyses seem to overestimate the dose rate in the D/W, especially in the early stages of the accident. The dose rate in the S/C, on the other hand, was underestimated by most of the analyses. The differences are presumably related to the assumed transport paths from the RPV to the PCV bypassing the pool, but also different scrubbing efficiency of fission products (this was not investigated in detail).

During the accident, monitoring posts (MP) recorded dose rates around the plant. In addition, activity was measured on the land and in the ocean in the following days. Calculations with atmospheric transport codes were performed by the GRS and the JAEA (Worldwide version of System for Prediction of Environmental Emergency Dose Information, WSPEEDI code) using inverse analysis to estimate the time and amount of FP releases based on these measurements. The method and the results are further explained later in this report in Chapter 6 and in Sogalla et al. (2019) and Katata et al. (2015).

Figure 2.7. **Comparison of calculation results against measured data: Unit 1 dose rate in the primary containment vessel**

A. Dry well CAMS B. Suppression chamber CAMS

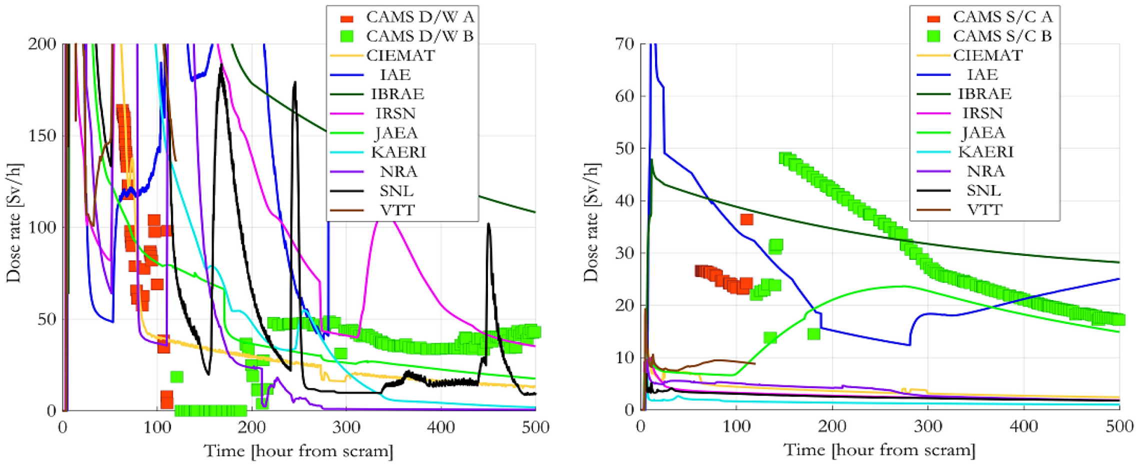

For unit 1, the comparison of the release calculated with the severe accident codes and the release based on the GRS and WSPEEDI analyses was relatively straightforward at the beginning of the accident because until around 35 hours (the estimated time of the start of unit 3's core degradation) there should not have been any other releases than those from unit 1. Figure 2.8 presents a comparison of the cumulative releases against the GRS and WSPEEDI analyses for Cs and I. First, it should be noted that results of the GRS and WSPEEDI codes tend to reach the same value at the time of venting and subsequent hydrogen explosion, although with about an order of magnitude difference in the case of I. Almost all calculations indicated a first release at around ten hours, when the PCV head flange was predicted to start leaking and FPs were released to the environment through the assumed leakage from the building. Nevertheless, these releases were lower than the value estimated by the GRS and WSPEEDI. The integral release after the PCV venting at 24.7 hours was predicted reasonably well in terms of the time and magnitude, within a range of about two orders of magnitude ($6 \cdot 10^{13}$ Bq-$5 \cdot 10^{15}$ Bq). Most calculations estimated that less than about 2% of cesium and 5% of iodine might have been released to the environment, although the best fit to the inverse calculations predicts Cs release between 0.5% and 1.0% and I release around 1%.

Figure 2.8. **Unit 1: Comparison of predicted cesium and iodine release [Bq] versus backwards analyses (GRS and WSPEEDI)**

A. Cesium B. Iodine

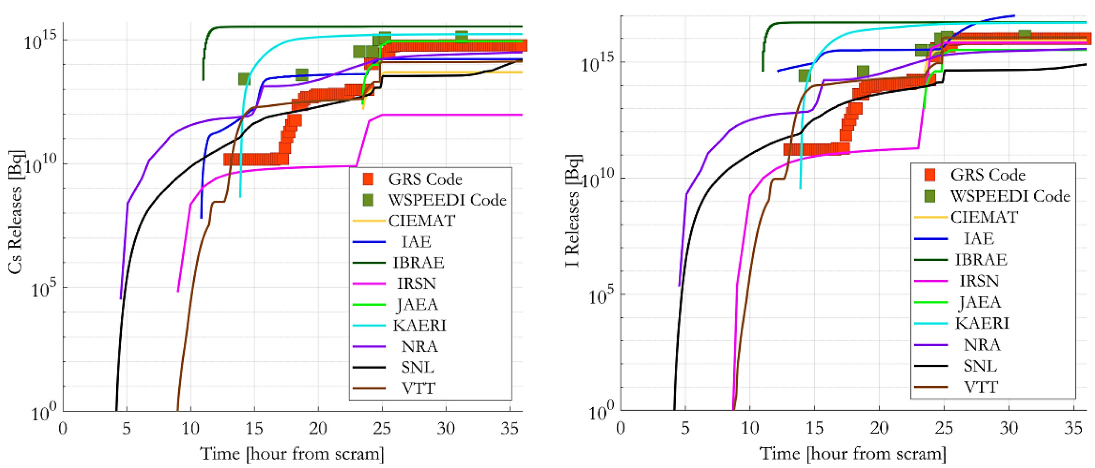

Chapter 3. Results of the unit 2 analyses

Overview of the unit 2 accident

The unit 2 accident is characterised by the protracted and unanticipated operation of the reactor core isolation cooling (RCIC) system for around 70 hours in a "self-regulating" mode, which is a phenomenon being pursued under separate research activities at the time of this report's publication. This situation developed, it is believed, when the uncontrolled full flow RCIC injection overfilled the reactor pressure vessel (RPV) up to the steam lines, allowing two-phase steam and water to be ingested into the RCIC turbine. Additionally, it was recognised that the torus room had become flooded by sea water, which removed heat from the suppression pool. It is also suspected that the water inside the suppression pool had thermally stratified, further complicating the analysis of this accident. After around 70 hours, the RCIC system finally failed, prompting operators to depressurise the RPV and attempt low-pressure injection using fire trucks. This action was ultimately unsuccessful in arresting core damage, owing to excessive PCV back pressure and eventual loss of water level in the RPV and core damage.

Thermal hydraulics and core degradation

The RCIC system remained in operation in unit 2 despite the loss of power. However, without power, it could not be controlled by the operators. When measurements resumed on 11 March around 10:00 p.m., the RPV water level was found to be above the maximum measurable value. Even though no direct evidence exists, it is suspected that the water level reached the main steam line (MSL), driving steam and water into the RCIC turbine. Overall, the RCIC worked for around 70 hours. The PCV pressure rise during this first accident period was found to be much lower than expected given the cumulative decay heat within the PCV, especially if compared to the accident progression in unit 3. In order to reproduce the too-low PCV pressure increase, additional phenomena had to be accounted for, such as temperature stratification in the suppression chamber (S/C) and additional heat losses due to a partial flooding of the torus room as a consequence of the tsunami. In general, all participants correctly predicted the main trends of the data, specifically the high RPV water level during the RCIC operation and the RPV pressure trend (Figure 3.1a). Some differences exist in the timing of the "turn-over point" in the pressure at around ten hours, which occurs slightly earlier than the time reported when the RCIC system was switched from taking water from the cooler condensate storage tank over to the warmer suppression pool water. A physical explanation for earlier-than-expected turn-over is not currently understood, although the increase in PCV pressure is consistent with the injection of warmer suppression pool water into the RPV. The PCV pressure increase (Figure 3.1b) was also captured well by most of the institutes, with a few outliers, such as the Japan Atomic Energy Agency (JAEA) and the Canadian Nuclear Laboratories (CNL) (early on). The pressure increase is the result of a balance of conditions driven by early tsunami flooding of the torus room, thermal stratification in the S/C water and evaporation from the hot surface of the S/C pool, and incomplete condensation of the RCIC water-steam mixture at elevated S/C pool temperatures.

After the failure of the RCIC at around 67 hours, the RPV pressure in unit 2 increased to the point where one safety relief valve (SRV) started to open (Figure 3.1), discharging steam to the S/C and reducing RPV pressure. As no water injection into the RPV was available, the RPV water level decreased further due to the out flow through the cycling SRV. Steam was discharged from the SRV into the S/C at a low position and the lower colder layer of water mixed with the hot layer on top, decreasing the surface temperature and thus condensing the steam and reducing the pressure. Detailed S/C models are required to represent this well. None of the submitted results using lumped parameter codes were able to properly match this phenomenon.

Figure 3.1. **Comparison of analyses results versus measurements for unit 2**

A. Reactor pressure vessel pressure | B. Dry well pressure

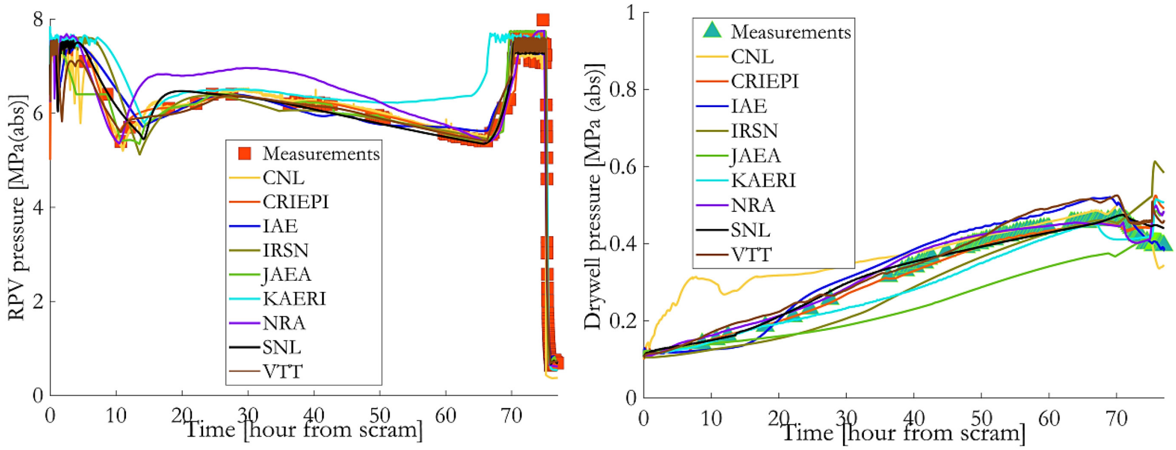

The core heat-up and degradation phase was predicted to start at around 75 hours at high RPV pressure or shortly after RPV depressurisation. There is consensus that core degradation began at this point and led to the pressure excursions in the RPV and the PCV – the so-called "RPV 3 pressure peaks period". The specific assumptions taken by the various analysts differ. However, all participants determined that the core degradation process led to non-condensable gas generation, melt relocation into the lower plenum of the RPV and consequential RPV failure (except for the Technical Research Centre of Finland [VTT]), melt release into the pedestal of the PCV, and in parallel fission product (FP) release from fuel/melt and transport into the PCV and further into the environment.

The first RPV pressure peak was attributed to steam and hydrogen production (Figure 3.2) during core heat-up. The hydrogen generation was predicted to be stronger in the next phase before the second RPV pressure peak due to more steam being available after reopening one SRV or due to material relocation within the RPV into a water pool. The PCV pressure trend until the end of the first peak was predicted well, even though the absolute values deviate by -0.1 MPa to +0.2 MPa from the measured values. The specific influence on the simulations of the different S/C nodalisations could not be separated out from other factors. Theoretically, the generation of steam and hydrogen has the same effect on the pressurisation of the RPV; however, hydrogen has a very different impact on the containment response, as steam released into a subcooled S/C may condense. At the time of SRV reopening (around 78.5 hours), the containment pressure showed a sharp increase due to gas/hydrogen released from the RPV (Figure 3.2).

During the second pressure peak, the RPV pressure increased dramatically (Figure 3.2a) and the PCV pressure followed consequently (Figure 3.2b). In order to replicate this simultaneous pressure rise, the calculations assume a partial SRV closure rather than a direct leakage from the RPV into the containment. Only four institutes (the Central Research Institute of Electric Power Industry [CRIEPI], the Institute of Applied Energy (IAE) and the Sandia National Laboratories (SNL), and to some extent the JAEA) show an RPV pressure trend similar to what was measured (Figure 3.2a), while the PCV pressurisation (Figure 3.2b) in general was not well predicted, except by the IAE and the JAEA. The pressure evolution during this period is assumed to be the result of direct slumping of core debris from the core into the lower plenum (for the IAE, JAEA and SNL). The pressurisation calculated by CRIEPI appears to be the result of water reflooding into the core region, which started early. At this time, CRIEPI computes a comparatively intact core, and steam is generated through quenching of the fuel rods. At the end of the second pressure peak, the PCV pressure reached its highest value, close to 0.8 MPa (Figure 3.2b), which was only reproduced well by the IAE and the JAEA. The maximum value, with a different timing, was reproduced by the Nuclear Regulation Authority (NRA) and the Radioprotection and Nuclear Safety Institute (IRSN). The high containment pressure remained for almost ten hours and, according to the analyses, was caused by large amounts of hydrogen released into the PCV (Figure 3.2c). Three institutes (the IAE, the IRSN and the NRA) predicted greater than 800 kg of hydrogen and were able to come close to predicting the measured PCV pressurisation. The other institutes that predicted lower hydrogen generation did not predict the large pressurisation of the PCV shown in the measurements. It was not analysed whether other phenomena may have caused such high PCV pressure during this period of the accident; however, direct leakages from the RPV into the dry well (D/W) of the PCV may be one possible phenomenon.

Figure 3.2. **Three reactor pressure vessel pressure peaks in unit 2**

A. Reactor pressure vessel pressure during core degradation

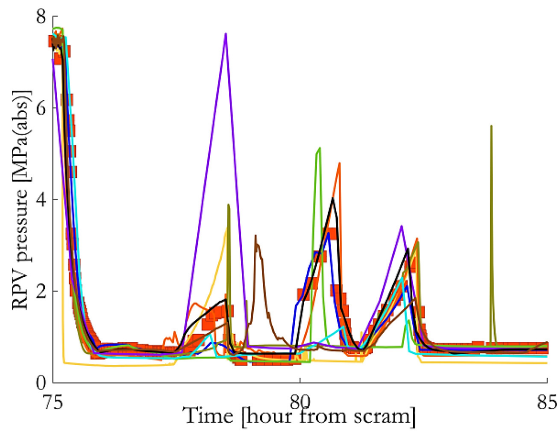

B. Primary containment vessel dry well pressure during core degradation

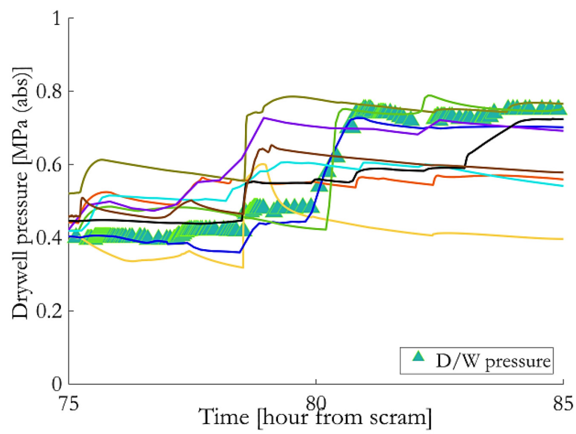

C. Hydrogen mass generated during core degradation

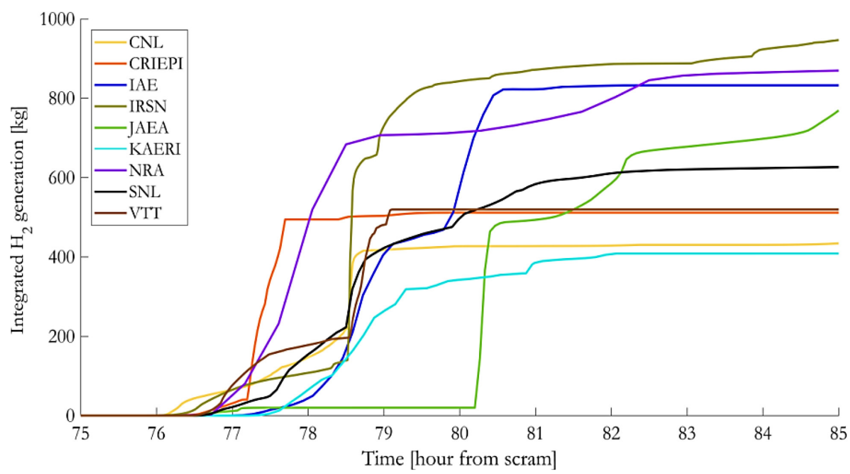

Note: Legend reported in Panel c.

During the third RPV pressure peak, complete closure of the SRV was assumed, as the PCV pressure did not increase in parallel. Almost all calculations reproduced the RPV pressure rise well, with the exception of the JAEA. The third pressure peak was likely caused by debris quenching in the lower RPV head associated with alternative water injection (AWI), which became available in unit 2 at about 75 hours at the earliest, according to measured data. In the analyses, the AWI data (timing, amount) have been widely varied to best match the measured plant parameters. The debris masses contained in the RPV lower head after this time period span a large range, from a few tonnes up to 160 tonnes; the RPV itself is still predicted to be intact at this point shortly after the three RPV peaks.

Since the time when the PCV pressure reached its highest value (at around 80.7 hours), the operators tried unsuccessfully to vent the PCV. A fast PCV pressure decrease was measured at about 89 hours (Figure 3.3), although the exact timing is unknown, due to a significant gap in data recording between the maximum value and the next low value. All institutes assumed that this pressure drop was due to a permanent failure/leakage occurring in the containment at 89 hours (typically at the head flange, but also at other locations as discussed in Table 3.1). The PCV failure/leakage reduced the pressure quickly (Figure 3.3) and in the long term, the PCV pressure was predicted to remain at a low level. A single PCV pressure measurement at about 118 hours indicates another possible peak, but this measurement was not considered in the analyses, as it seemed likely to be erroneous. In addition to the PCV failure at the head flange, two institutes (the CNL and the JAEA) also model an S/C failure in the pool region. The S/C failure is predicted based on evidence obtained at the plant from measurements and investigations that confirmed the water level in the torus room and in the torus itself to be nearly identical (TEPCO, 2014).

Figure 3.3. **Unit 2 primary containment vessel dry well pressure during a longer term**

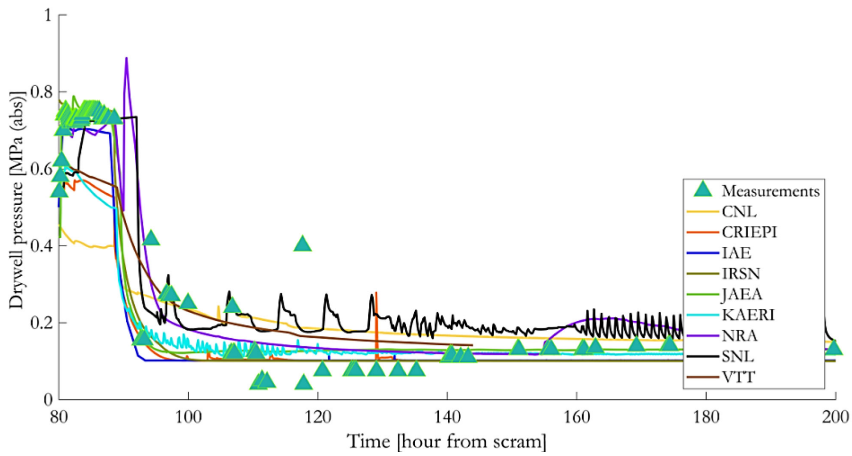

Table 3.1. **Unit 2 primary containment vessel and reactor pressure vessel (RPV) lower head failure and debris mass released from the RPV**

	CNL	CRIEPI	IAE	IRSN	JAEA	KAERI	NRA	SNL	VTT
LH failure time (hours)	104.57	129.0	93.36	95.32	92.0	441.19	85.8	83.0	–
LH failure mode	Penetration failure	Penetration ejection	RPV creep	Penetration failure	Penetration failure	Penetration failure	Penetration failure	Penetration failure	No failure
PCV failure (hours)	89.0	88.54	88.55	88.57	87.0//89.2	88.89	N/A	N/A	89.0
PCV failure mode	Head flange leakage	Head flange leakage	Head flange leakage	X-6 penetration leakage	X-6 penetration/ head flange	Head flange leakage	N/A	N/A	Head flange leakage
S/C water leakage (hours)	89.0	N/A	N/A	N/A	88.0	N/A	N/A	N/A	N/A
Total masses in pedestal (tonnes)	78	399[1]	35	16	N/A 0	186	157	111	N/A 0

1. Sandia National Laboratories is a multi-mission laboratory managed and operated by National Technology & Engineering Solutions of Sandia, LLC, a wholly owned subsidiary of Honeywell International Inc., for the US Department of Energy's National Nuclear Security Administration under contract DE-NA0003525. SAND2018-8356 R.

Note: LH: lower head; PCV: primary containment vessel; S/C: suppression chamber.

Due to the large mass of debris in the lower head and the relatively low AWI into the reactor vessel, the lower head was predicted to fail between 83.0 hours and 129.0 hours for most calculations, except for Korea Atomic Energy Research Institute (KAERI), with a very late failure at 441 hours, and the VTT, without RPV failure (Table 3.1). The debris mass released into the pedestal for all calculations except KAERI varies from 16 tonnes for the IRSN up to 161 tonnes for the NRA. The molten core concrete interaction (MCCI) radial/axial erosion of the cavity/pedestal, and continuous release of non-condensable gases depend strongly on the modeling assumptions. After the RPV failure and melt release, CRIEPI, the NRA and the SNL predicted unterminated concrete erosion; KAERI also predicted this condition, but at a much later point in time. None of the other calculations predicted an MCCI. The prediction of little or no MCCI seems to be consistent with evidence found in Tokyo Electric Power Company's (TEPCO) plant investigations of unit 2.

Fission product release and behaviour

In unit 2, a large release from the damaged fuel of noble gas (NG) (Xe), Cs and I, in general above 80% of the initial mass, was predicted by the calculations during the early core degradation phase prior to the first RPV pressure peak. Most calculations predicted that fission product (FP) release from fuel started at around 75 hours and was almost complete at the end of the second RPV pressure peak (around 82 hours). Only KAERI predicted a much slower release of NG and volatile FPs from the fuel. The predicted FP release from fuel for Xe and I are provided in Figure 3.4.

Figure 3.4. **Unit 2 mass fraction of fission product released from fuel a) Xe and b) I**

A. Xeron (Xe)

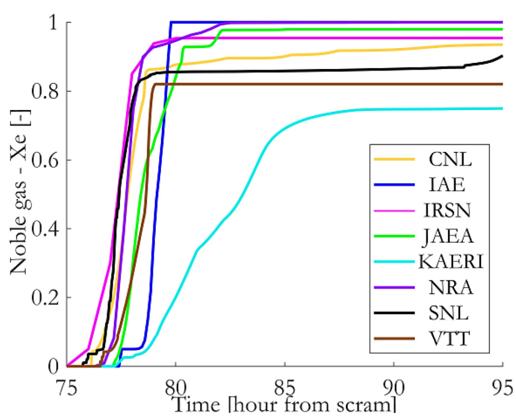

B. Iodine (I)

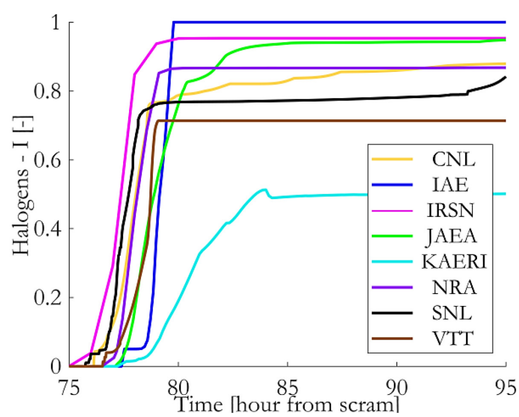

Because FP release from fuel was predicted to start after the RCIC failed and no leak path was assumed connecting the RPV to the D/W, then from the point of RCIC failure up until RPV failure, the SRVs were the only modelled connection path from the RPV to the PCV. Volatile FPs were predicted to have been transported from the RPV through an SRV and its sparger into the S/C. Predictions of FP behaviour in the containment were calculated for the D/W and S/C and divided into airborne FPs (not presented in this report), deposited FPs on structures (wall, piping and floor), and FPs in the water.

NGs were released to the S/C through the operating SRV during the RPV 3 pressure peaks period and partially transferred to the D/W through operating S/C vacuum breaker(s). Of major interest to the FP behaviour in containment are the deposition of Cs and I on D/W structures and the amount of Cs and I solved in the S/C water (Figure 3.5). The predicted Cs and I deposition on the D/W structures (Figure 3.5a and b) for most calculations is a final deposition of less than 3%, with some exceptions. The IAE predicted about 23% of I deposited on structures and the CNL predicted about 7%. The NRA predicted a strong initial peak in the deposition of both Cs and I, but subsequently calculated that this deposited mass was revolatilised within the next 40 hours. The predictions for Cs and I retention in the S/C water pool by pool scrubbing (Figure 3.5c and d) were very different across the calculations, from less than 10% (KAERI) to about 75% (IRSN) in the long term. The JAEA showed an even larger peak value, about 90%, during core degradation, which decreased due to leakage assumed at the bottom of the S/C. The variations in the predictions were caused by differences in the retention of Cs and I in the RPV, and by the fact that some calculations modelled water leakages from the S/C to the torus room (the CNL and the JAEA). The calculations by the CNL, the JAEA and the NRA showed a continuously decreasing mass of Cs and I retained in the S/C water in the longer term due to the water leakages from the S/C. Additionally, less contaminated water injected by AWI into the RPV flows over from the D/W, which diluted the S/C water inventory.

Figure 3.5. **Unit 2 mass fraction of fission products deposited on structures in the dry well and solved in water in the suppression chamber**

Deposited on structures in the dry well

A. Cesium (Cs)

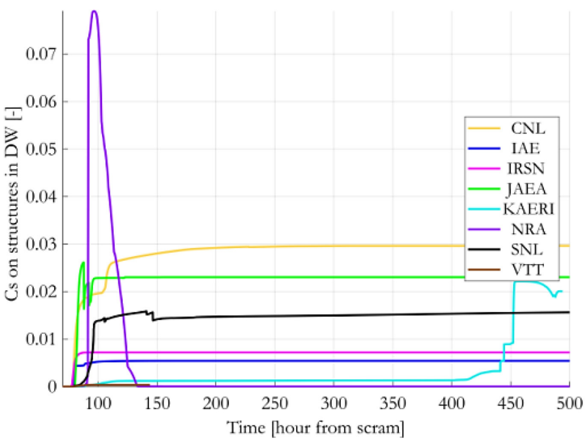

B. Iodine (I)

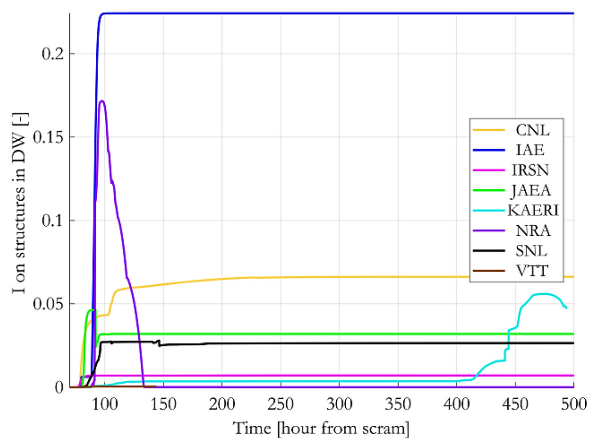

Solved in water in the suppression chamber

C. Cesium (Cs)

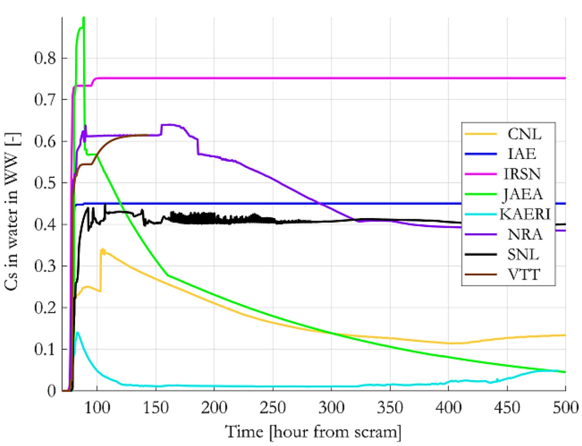

D. Iodine (I)

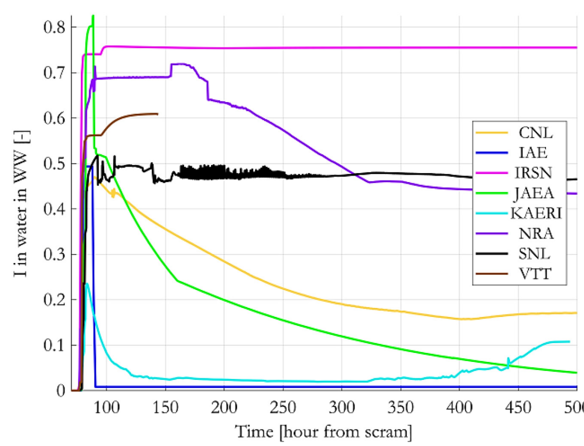

In unit 2, the analyses predicted that the main FP release into the PCV occurred during the RPV 3 pressure peaks period and later into the environment, when the PCV depressurisation started, at about 89 hours. The release path of airborne FPs was typically assumed through a leakage of the PCV head flange, into the reactor well and further through the fifth floor of the intact reactor building upper part and out the failed blowout panel into the environment (see Table 3.1).

Unit 2 had relatively detailed containment air monitoring system (CAMS) measurement data in the D/W and S/C (two systems A and B each) available during the accident. During the expected core degradation period, starting about 75 hours after scram, dose rate measurements increased quickly, from 10 Sv/h and 3 Sv/h to around 100 Sv/h and 10 Sv/h for the D/W CAMS (Figure 3.6a) and S/C CAMS respectively (Figure 3.6b). The FP release from fuel predicted by the calculations started at about the same time as the CAMS data, for both the D/W and S/C, showed this first large increase. This is seen as a confirmation of the analyses. The first FP releases were through the operating SRV into the S/C. The S/C CAMS measured a peak dose rate at about 80 hours (Figure 3.6b). The peak appears to be overpredicted by most of the calculations by four to five times, but this is still within the uncertainty of the conversion methodology (estimating an equivalent dose from the predicted FPs in the D/W or S/C). With regard to the D/W CAMS measurements, the predicted results for most calculations are in better agreement with the measurements, but overpredictions are also seen (Figure 3.6a). Dose in the D/W before the RPV failure is assumed to be caused by the transport of NGs and aerosols from the S/C through the vacuum breakers. The dose measured in the D/W increases by another peak at ~95 hours, which might indicate RPV failure.

Figure 3.6. **Comparison of analyses results against measured data in the unit 2 dose rate in the primary containment vessel**

A. Dry well CAMS

B. Suppression chamber CAMS

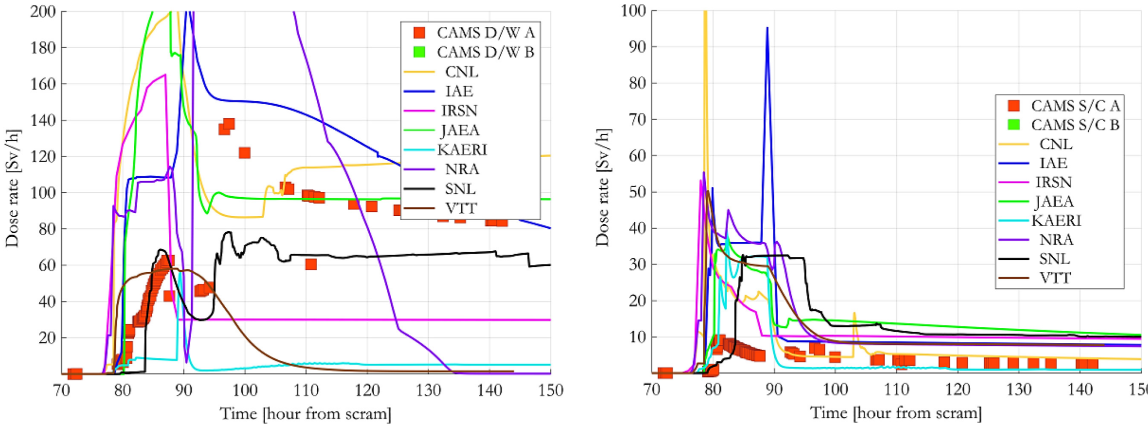

Differences in the calculations were pronounced for the airborne release of Cs and I into the environment (Figure 3.7). The final predicted values for Cs release were lower than 0.1% (the IRSN and the IAE), about 0.1% (the VTT and the JAEA) and 1.5-5% (all others). For I, the split of the results is different: less than 0.5% (the IRSN and the NRA), about 2-5% (the JAE, KAERI and the SNL), 9% (the CNL), and about 17% (the IAE). Almost all NGs were released through PCV leakages into the environment within about 10 hours after the PCV failure, at about 89 hours.

The predicted FP release source term from the severe accident (SA) code calculations was compared against inverse analyses provided by the GRS and WSPEEDI (Worldwide version of System for Prediction of Environmental Emergency Dose Information). During the RPV 3 pressure peaks period and the strong core degradation in unit 2, the wind was blowing towards the land. The strong releases (dose rates) measured during this time were attributed to releases from unit 2 (Sogalla et al., 2019; Katata et al., 2015), as the main core degradation periods in the other two units occurred much earlier. The mechanisms or release paths from the unit 2 containment are still unclear. In general, airborne releases from unit 2 are expected to occur when the PCV pressure is high (likely through PCV head flange leakage). Unit 2 PCV venting was attempted, but reported unsuccessful.

Figure 3.7. **Unit 2 mass fraction of fission products released into the environment**

A. Cesium (Cs) B. Iodine (I)

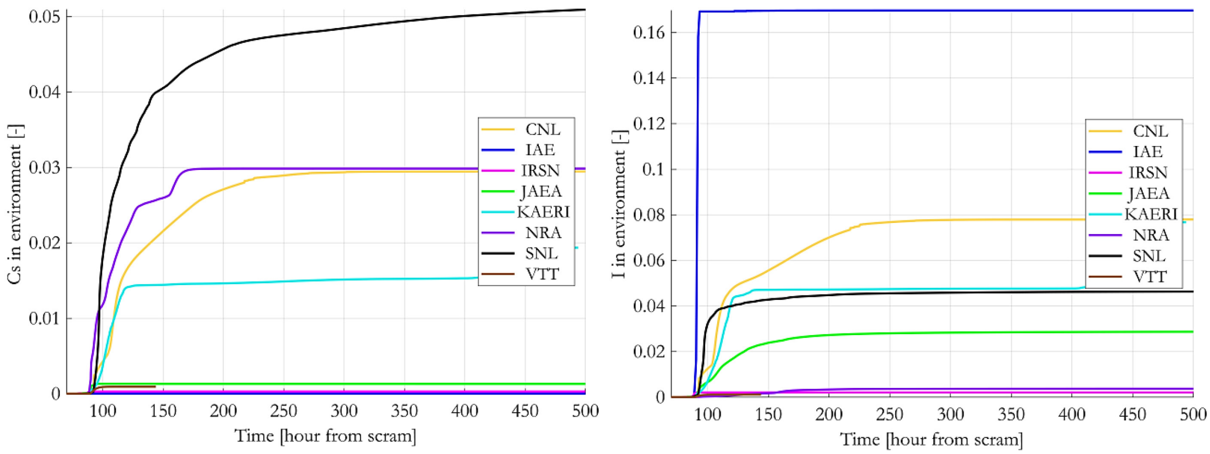

Figure 3.8 shows a comparison of Cs releases predicted by the calculations versus the GRS and WSPEEDI backwards analysis during and after the three RPV pressure peaks period (up until 120 hours); the RPV pressure is also included in the figure for comparison (green triangles). The integrated release data of the GRS and WSPEEDI analyses is only available starting at around 75 hours; earlier releases are not considered.

Figure 3.8. **Unit 2 comparison of predicted cesium and iodine releases [Bq] versus backwards analyses (GRS and WSPEEDI) and RPV pressure (RPV 3 pressure peaks period until 120 hours)**

A. Cesium (Cs) B. Iodine (I)

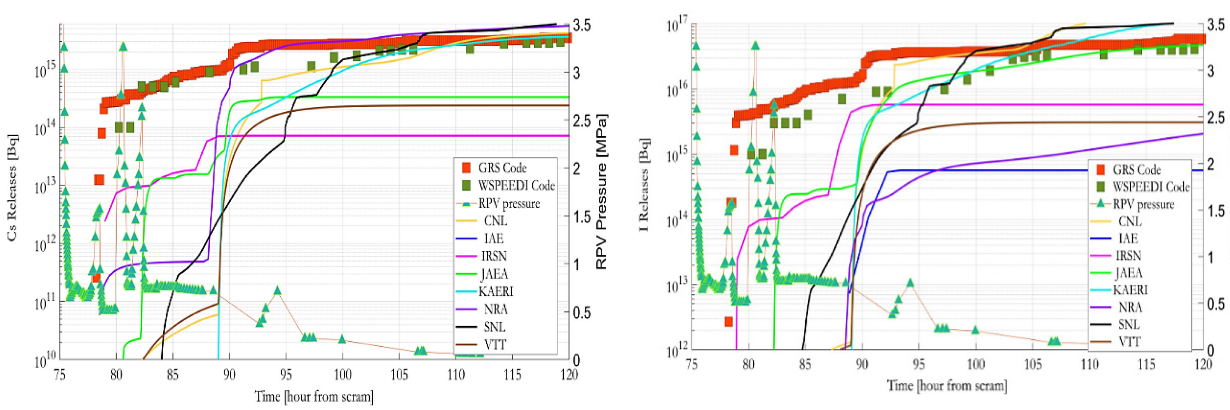

Even though all institutes predicted the start of the FP release from the fuel at the time of the first RPV pressure peak, only four (the CNL, the IRSN, the NRA and the VTT) predicted an increase in the radio nuclide release to the environment at this time as well, which is suggestive of a small leakage from PCV through the reactor building upper part (likely the head flange) to the environment. These predicted results are still much lower than the values estimated by the GRS and WSPEEDI analyses.

For the initial release (at ~77 hours), the NRA and the IRSN predicted release values around 1.0 E+11 – 1.0 E+12 Bq for Cs and one order of magnitude more for I (the IRSN only), while the CNL and the VTT showed releases starting at about 82 hours, but at several orders of magnitude lower. Spikes in Cs release were also predicted by the JAEA (~1.0E+13 at 82 hours) and the SNL (~1.0 E+11 at 84 hours). The IRSN and NRA calculations predicted a large PCV pressure at ~79 hours coinciding with the end of the first RPV pressure peak, much earlier than measured. This might be the reason for the predicted early FP release from the PCV. All institutes showed significant FP releases from ~89 hours on when the PCV depressurisation starts and PCV head flange leakage was assumed (see Table 3.1). These release predictions were almost in accordance with another significant increase of the integral releases estimated by the GRS backwards calculation, while the WSPEEDI calculation showed this increase later, between ~95 and 105 hours. After the PCV had completely depressurised at ~95 hours, results by the CNL, the JAEA, KAERI, the NRA and the SNL showed a continuous increase of the releases (though with decreasing slope), while in all other calculations, the releases stopped. At ~120 hours the agreement between the estimations by the GRS and the WSPEEDI analyses and the predicted releases from the calculations is not total. For Cs, about half of the calculation results were still significantly below the values that the GRS and WSPEEDI estimated, while others were in agreement (the CNL and KAERI) or slightly above (the NRA and the SNL). The result was similar for I releases, with most calculations yielding results a few orders of magnitude below the GRS and WSPEEDI estimates, one in agreement (JAEA) and three slightly above (the CNL, KAERI and the SNL).

Chapter 4. Results of the unit 3 analyses

Overview of the unit 3 accident

The unit 3 accident is characterised by normally functioning heat removal from the reactor pressure vessel (RPV) in the first 35 hours of the accident, first by the reactor core isolation cooling (RCIC) coolant injection system, then subsequentially by the much higher capacity high pressure coolant injection (HPCI). While these systems performed normally, their operation could only serve to replace water lost from the RPV and to move heat from the reactor fuel to the suppression chamber (S/C) water and the primary containment vessel (PCV) atmosphere. The PCV pressure increase due to steady steam injection was controlled in a later accident phase by spray activation in the S/C. During this first accident period, all of the participants predicted the main signatures in the RPV and PCV reasonably well. After the HPCI was stopped, unit 3 experienced a period of about ten hours with no coolant injection into the reactor, which is thought to have caused the reactor water level to drop below the bottom of active fuel. Most of the analyses show that core degradation started during this time, and was accompanied with hydrogen generation, causing further pressurisation of the PCV. The period after reactor depressurisation is postulated to have occurred by spurious operation automatic depressurisation system (ADS), at about 42 hours, up until the hydrogen explosion in the unit 3 reactor building, at 68 hours, was characterised by a number of attempts by operators to depressurise the containment and inject water into the RPV using fire trucks.

Unit 3 thermal hydraulics and core degradation

Unit 3 had direct current (DC) power available after the tsunami, and consequently, a large amount of measured data is available (e.g. water level values, RPV pressure, PCV pressure and lower head temperature) for long periods of time. Several containment vent actuations were attempted as well as coolant injections by means of the RCIC, the HPCI and the alternative water injection, with some interruptions. The timings of the coolant injection to the reactor as well as containment vent attempts were recorded by the operators and used by the analysts as boundary conditions, depending on their interpretation of the accident. Even though the approximate timing of the venting and coolant injections are known, the actual success of these operations is still considered uncertain.

For the first 20 hours after the accident initiation, the unit 3 core was cooled by the RCIC, pressure in the RPV was regulated by the safety relief valves (SRVs; see Figure 4.1a) and the water level in the reactor stayed relatively constant at a high level above the top of active fuel. During this time, the containment pressure (Figure 4.1b), increased continuously, which is assumed to be due to thermal stratification in the suppression pool, leading to high pool surface temperature. After about 20 hours, the RCIC stopped automatically due to high pressure in the suppression pool. As a result, the water level in the reactor started to decrease. The HPCI system started about one hour later due to the low water level in the reactor. After the HPCI operation started, the water level in the reactor increased again while the pressure in the reactor decreased sharply due to large amounts of steam extraction by the large capacity HPCI turbine. The calculations assumed that the HPCI performance started to degrade at around 30 hours. The HPCI was manually stopped at 36 hours by the operators, after which they attempted to depressurise the RPV by opening the SRVs, which eventually failed. Most of the calculations could reproduce the RPV and PCV pressure trends in a satisfactory way during this time.

After coolant injection by the HPCI stopped, there was a period of some ten hours with no coolant injection into the reactor. During this time, the water level in the reactor dropped below the bottom of active fuel and the reactor pressure increased rapidly. Most of the calculations predicted that major core degradation started during this time, accompanied by hydrogen generation (Figure 4.2), resulting in an increase in the dry well (D/W) pressure up to 0.4 MPa. The reactor pressure reached the set point of the SRVs, and after several hours of high RPV pressure, the reactor is hypothesised to have become depressurised by the ADS at 42 hours. The ADS was thought to have accidentally activated due to high D/W pressure, which is believed to be the result of the continuous hydrogen and steam generation in the RPV. The ADS included simultaneous activation of 6 SRVs producing a PCV pressure increase up to 0.6 MPa and confirming that this first RPV vent activation was successful. The containment pressure was decreased by venting from the S/C gas space soon after the ADS activation at around 42.5 hours.

Figure 4.1. **Unit 3 reactor pressure vessel pressure and primary containment vessel pressure**

A. Reactor pressure vessel

B. Primary containment vessel pressure

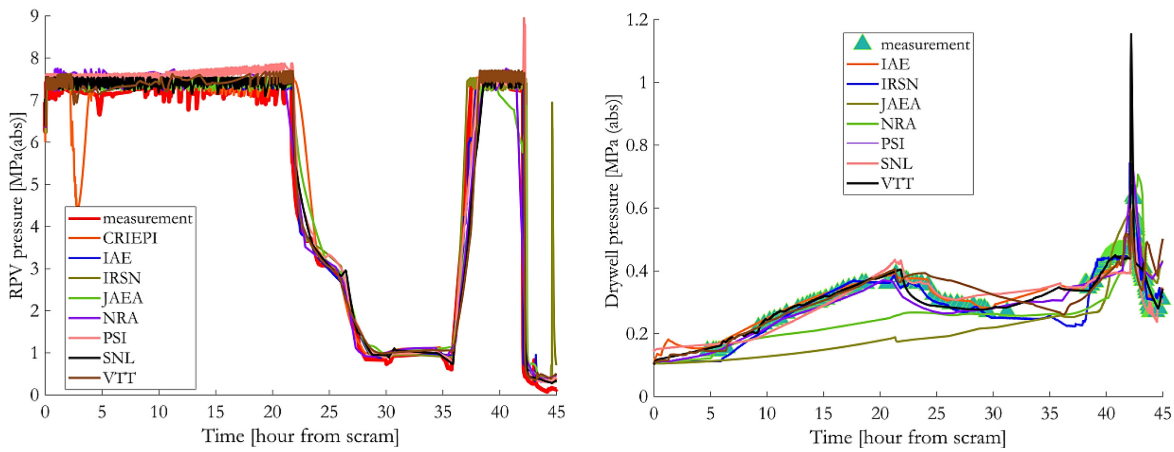

Figure 4.2. **Unit 3 in-vessel hydrogen generation**

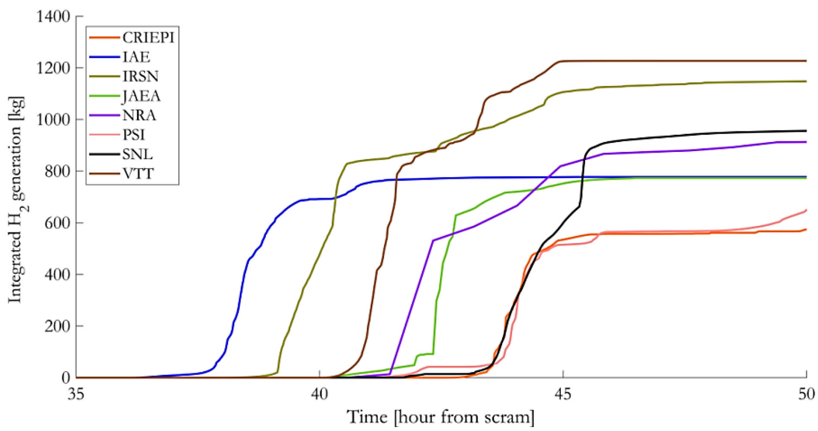

The period after reactor depressurisation at 42 hours until the hydrogen explosion that took place in the unit 3 reactor building at 68 hours involved repeated attempts by the operators to depressurise the containment and inject water by means of fire trucks. As presented in the latest Tokyo Electric Power Company (TEPCO) reports, the only other confirmed vent occurred at 45 hours (TEPCO, 2017a). Most of the calculations predicted major core degradation and core slumping during this time, eventually leading to the failure of the RPV. The timing and mode of the RPV failure assumed/predicted by different calculations are shown in Table 4.1. The timing of the vessel failure varies some depending on the boundary conditions and codes used, with most participants within a range of 43-58 hours, with two later predictions at 73 hours (the Paul Scherrer Institute – PSI) and 102 hours (Central Research Institute of Electric Power Industry – CRIEPI).

Table 4.1. **Unit 3 assumed lower head failure time and mode of failure; total debris mass released from the reactor pressure vessel to the containment**

	CRIEPI	IAE	IRSN	JAEA	NRA	PSI	SNL	VTT
Time of failure	101.95	55.20	55.37	46.48	49.40	73.05	58.03	43.30
Mode of failure	Penetration failure	Creep failure	Creep failure	Vessel melt	Penetration failure	Penetration failure	User specified	Penetration failure
Mass in pedestal (tonnes)	244	105	51	188	65	21	205	224

After the hydrogen explosion at 68 hours, the containment pressure remained high until about 130 hours (Figure 4.3). This is partly due to further gas generation by the oxidation of corium and metallic structures in the containment, as predicted by several calculations, and partly due to steam generation from the continuous water injection. Due to the coolant injection, several calculations predicted that the water level in the PCV reached the main steam line penetration in the dry well by the end of the calculation. The possibility of this has been observed in the unit 3 plant inspections, as a water leakage has been observed at the level of the main steam line. Most of the calculations reproduced the containment pressure trend during this time relatively accurately.

Figure 4.3. **Unit 3: A. containment pressure; B. concrete erosion depth; C. ex-vessel hydrogen generation**

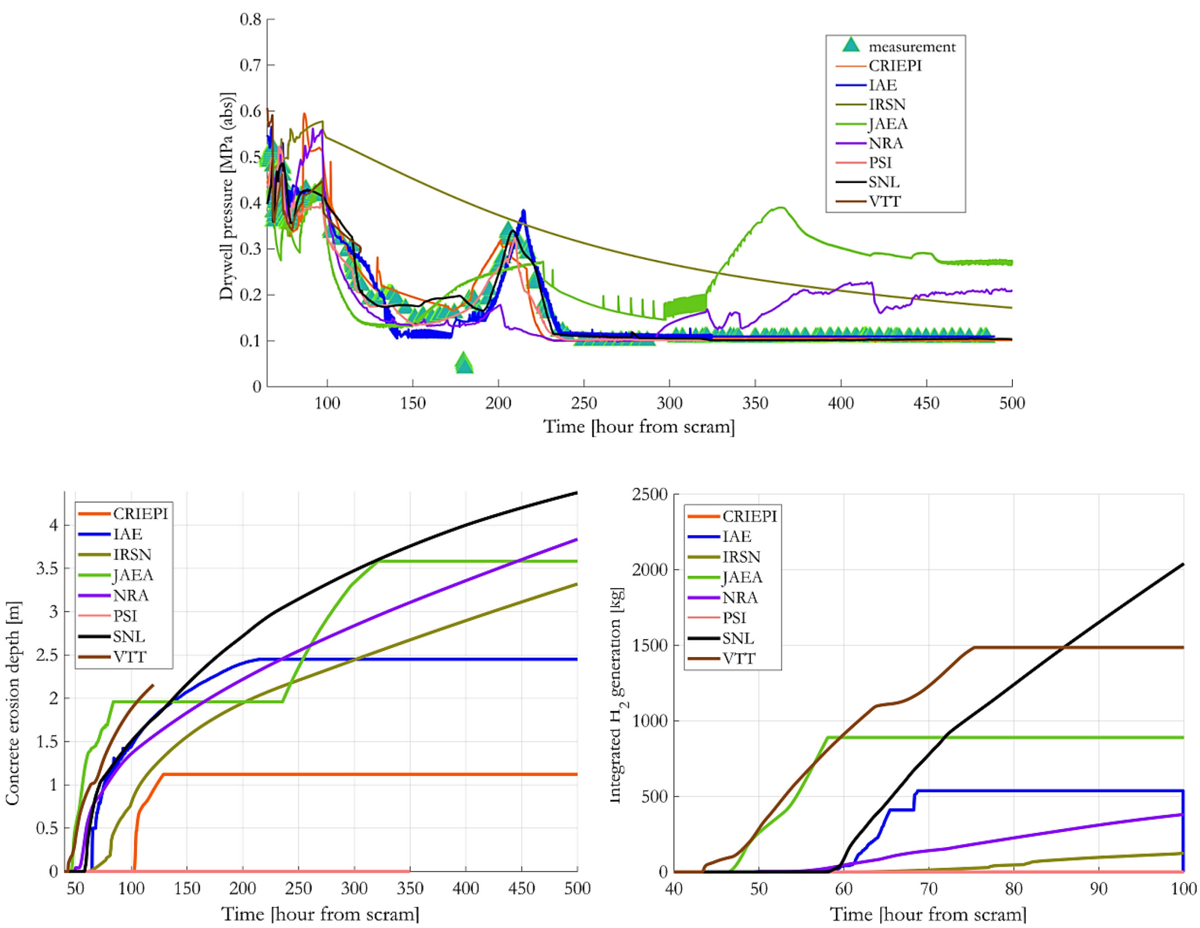

From the time of vessel failure to the end of the simulation (~500 hours), the majority of the calculations predicted a large mass of debris discharged into the containment, followed by continuous molten core concrete interaction (MCCI) (Table 4.1). A large amount of debris on the containment floor has been confirmed through unit 3 plant inspections with video cameras mounted on submersible robots (TEPCO, 2017b). Three calculations show smaller amounts of material released to the containment. The variation in the results of the calculations was large for both the timing and the magnitude of the corium release from the reactor pressure vessel to the containment. TEPCO's latest investigations of unit 3 containment (TEPCO, 2017b) indicate that the debris mass in the containment is likely closer to the higher values given by the analyses than the lower ones. All of the calculations except for one (the PSI) predict that the MCCI started once the corium was released to the containment floor. However, the MCCI in the unit 3 containment has not been confirmed nor disproved by plant investigations.

Fission product release and behaviour

The core degradation accompanied by fission product (FP) release from the fuel was predicted to have initiated prior to the RPV depressurisation by the ADS in most of the analyses. The volatile FP release from the fuel was predicted to progress rapidly once the core degradation began (Figure 4.4). Cs and I (Figure 4.4b) release was very similar to that of Xe (Figure 4.4a). Most of the calculations predicted a similar profile of a fast release, sometimes in steps following the core degradation progression, up to an asymptotic high value bracketed between 90% and 100% of the element inventory. A slightly lower total release of about 80% was calculated by the PSI and the SNL for I.

Before the ADS, FPs were transported to the suppression pool through SRV spargers and were assumed to be scrubbed efficiently. As a consequence, large amounts of fission products accumulated in the suppression pool. Noble gases (NGs) were transported through the pool and remained partly in the gas space of the S/C, and were partly transported to the dry well as the S/C pressure increased.

The distribution of the FPs within the PCV was influenced by the assumptions of the analysts in modeling RPV leakages to the D/W. As presented in Table 4.2, some of the calculations assumed direct leakages from the RPV to the D/W (such as primary loop recirculation or recirculation pump seal leakage), which allowed FPs to be transported from the RPV to the containment without being scrubbed in the suppression pool. Two calculations (the JAEA and the Technical Research Centre of Finland [VTT]) assumed early leakage from the RPV through a pump seal. Other calculations predicted direct leakages from the RPV to the D/W at around the time core degradation started in Unit 3. The SNL calculation, as in its unit 1 analysis, predicted a main steam line failure around the time core degradation starts and subsequent large releases of FPs to the dry well.

Table 4.2. **Unit 3 assumed leakages from the reactor pressure vessel into the primary containment vessel and timing**

Hours

	CRIEPI	IAE	IRSN	JAEA	NRA	PSI	SNL	VTT
RPV leak (MSL creep)							42.30	
RPV leak (SRV leak)		43.00			42.20			
RPV leak (pump seal)				5.00				6.33
RPV leak (TIP leak)				39.75	41.90			

Notes: RPV: reactor pressure vessel; MSL: main steam line; SRV: safety relief valve; TIP: transverse instrumentation probe.

Once in the D/W, the FPs may be transported into the reactor building if the containment integrity is compromised. All the calculations assumed that once the containment pressure increased to a certain level, the dry well head would lift due to elastic stretching of the head bolts, opening a gap at the D/W head flange and producing leakage from the D/W into the reactor well. The reactor building was not designed as a pressure-tight structure and, as such, releases to the reactor building were followed by a minor release to the atmosphere through building leakage. Once the hydrogen explosion in unit 3 occurred (~68 hours), a large direct leakage path from the reactor building to the environment was created.

Figure 4.4. **Unit 3 mass fraction of fission product released from fuel**

A. Xeron (Xe)

B. Iodine (I)

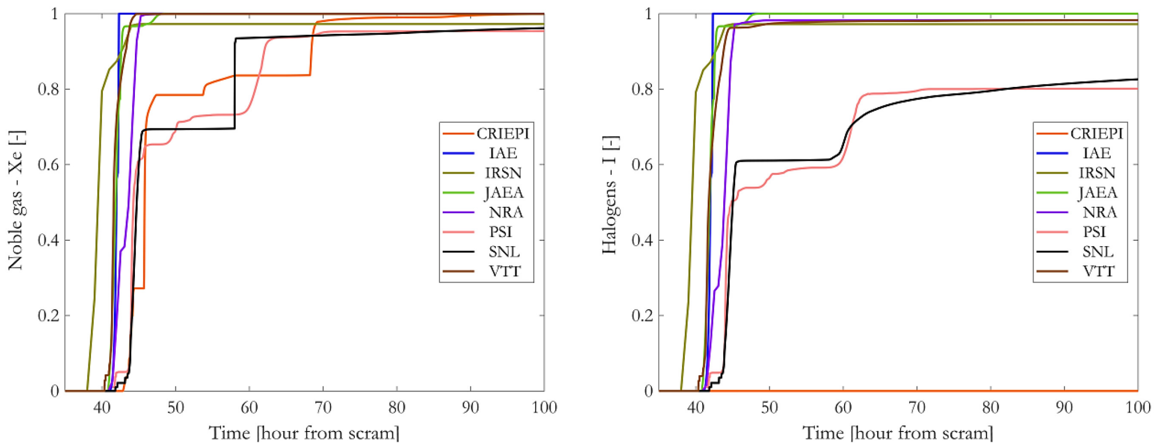

Large fractions of Cs and I were predicted to be retained in the suppression pool water (Figure 4.5) in all of the calculations. Several calculations showed a large fraction of Cs in the RPV due to deposition of Cs compounds on the reactor walls, either by chemisorption or aerosol deposition. A fraction of FPs was also calculated to be deposited on the walls of the dry well (Figure 4.5a and b). Note that the results of one analysis (the SNL) are above the scale of y-axis shown in Figure 4.5a and b.

The dose rates in the D/W and S/C of the containment were measured during the accident by the containment air monitoring system (CAMS). In unit 3, CAMS measurement data were available around the time of the hydrogen explosion (60-70 hours), and from 150 hours to the end of the simulation time (500 hours). The timing and magnitude of the CAMS measured dose rates were compared with those predicted by the code calculations. For the comparison, the concentration of the different radionuclides in the containment as calculated by the severe accident codes was converted to a dose rate considering the specific geometry of the CAMS measurement (Uchida et al., 2021). Calculations that assumed an early and large leakage from the RPV to the D/W and subsequent large deposition of fission products on the D/W structures tend to overpredict the dose rate in the dry well significantly. The other calculations, which assumed a smaller early leakage from the RPV to the D/W, seemed to predict the increase in the dose rate in the D/W too early; however, given the lack of dose rate measurements before 60 hours, nothing conclusive can be determined. The calculations that did not assume any direct release of FPs from the RPV to the D/W before 60 hours underestimate the dose rate in the D/W by a large extent. Based on the dose rate measurements at around 60 hours, about 5% of Cs and I was in the D/W at this time, mainly as a result of a direct transport of Cs and I from the reactor vessel to the D/W.

Figure 4.5. **Unit 3 mass fraction of fission products deposited on structures in the dry well and solved in water in the suppression chamber**

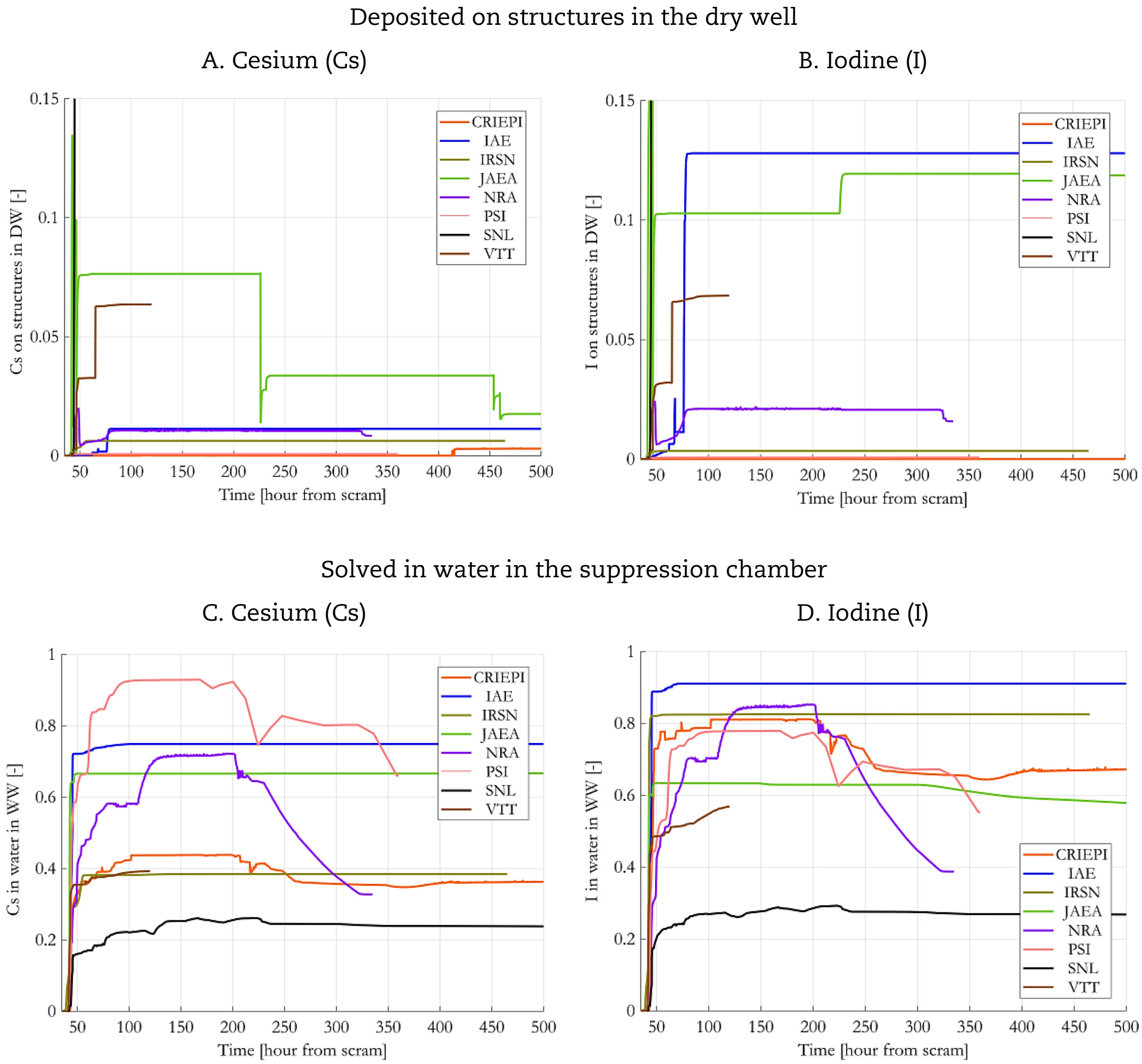

Comparison of the calculation results with the S/C CAMS measurements shows that almost all calculations overestimate the dose rate in the suppression chamber. Note that some of the results are not visible in Figure 4.6 because their values are higher than the y-axis scale. Possible reasons for the overestimation may be a different S/C water level than assumed by the conversion method or other phenomena, such as wall washing, that increase FP remobilisation from the structures to the pool that are not accounted for in the code calculations. Overestimation may also be due to unrealistically high calculated pool scrubbing efficiency of the FPs in the suppression pool.

The calculations predicted that the main FP release to the atmosphere in unit 3 took place during the first two containment vents and at the time of the hydrogen explosion. In addition, one calculation (the SNL) showed a continuous release of Cs and I through a D/W head flange leak after the hydrogen explosion, and two calculations (the JAEA and the NRA) showed a considerable release at around 220 hours in connection with the pressure increase in the containment at that time (Figure 4.7).

Figure 4.6. **Comparison of calculation results against measured data for the unit 3 dose rate in the primary containment vessel**

A. Dry well CAMS B. Suppression chamber CAMS

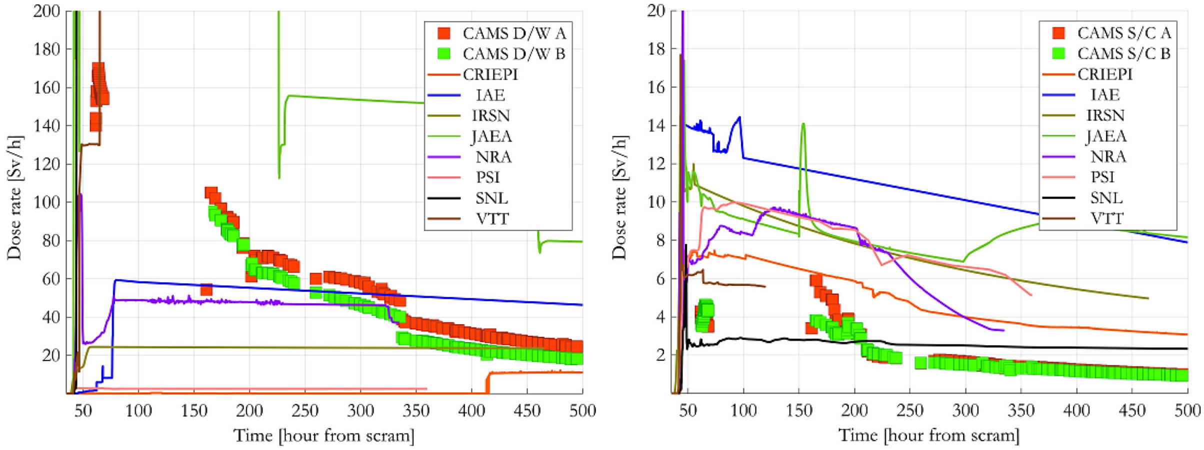

Figure 4.7. **Unit 3 mass fraction of fission products released to the atmosphere**

A. Cesium (Cs) B. Iodine (I)

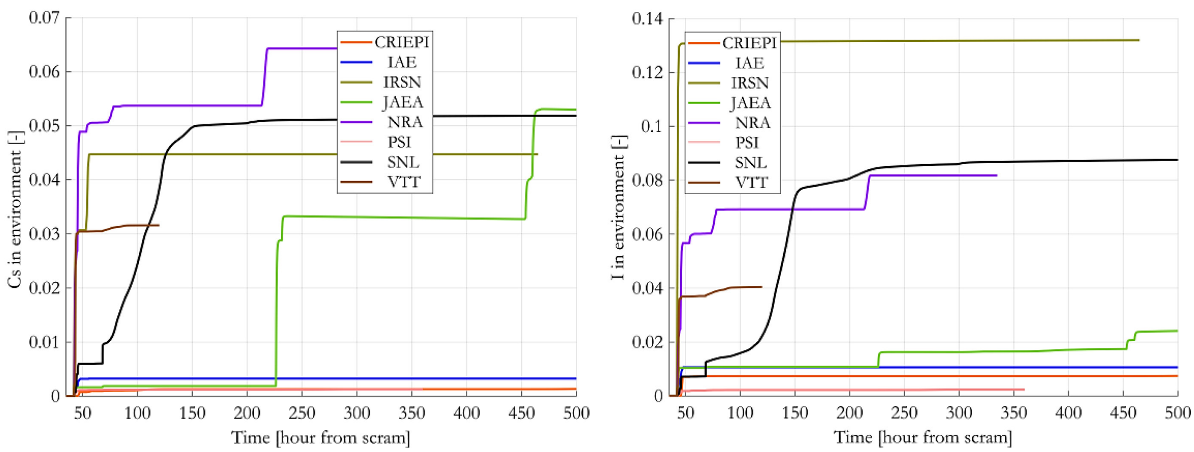

About 80-100% of the NGs were released to the atmosphere up until the hydrogen explosion at 68 hours. The calculations vary in their predicted timing of the release, depending on the accident progression and the assumed transport path for the FPs. Two calculations (the JAEA and the NRA) showed continued release of NGs after this time. Differences in the calculations are more pronounced for the release of Cs and I. Three calculations (the IRSN, the NRA and the VTT) show a fast release of 3-5% of Cs to the atmosphere during the first containment vent that occurred shortly after the ADS actuation. The majority of the calculations assumed transport of Cs from the RPV to the containment through SRV cycling with efficient scrubbing of Cs in the suppression pool, and a subsequent release of less than 0.5% Cs until the hydrogen explosion. Iodine release was similar, with the release fraction being on average slightly higher than that of Cs. One calculation (the IRSN) predicted a fast, high release of I at the first containment vent, reaching a total of 13%. The other calculations fell into two groups: three calculations (the NRA, the SNL and the VTT) predicting I release to the environment of 4-9%; the remaining four calculations predicting about 2% or less.

Unit 3 is a special case, as a fraction of the gas in the unit 3 containment was transported to the unit 4 reactor building through the common stack during attempts to vent unit 3. A hydrogen explosion took place in the unit 4 reactor building about 19 hours after the explosion in unit 3. TEPCO analysis shows that the hydrogen that caused the explosion in unit 4 was transported from unit 3 through the ventilation channel during venting of the containment of unit 3 (Uchida et al., 2021). According to TEPCO's analysis, approximately 20-35% of the vented gas could have been diverted to the unit 4 reactor building during the vent actions. This transport path is not accounted for in the Benchmark Study of the Accident at the Fukushima Daiichi Nuclear Power Station (BSAF) calculations and would reduce the release to the atmosphere due to the deposition of FPs in the ventilation lines and in the unit 4 reactor building.

Figure 4.8 shows a comparison of cumulative releases of Cs and I as predicted by the severe accident code calculations and the releases estimated by the GRS and WSPEEDI (Worldwide version of System for Prediction of Environmental Emergency Dose Information) backwards analysis based on environmental measurements and distribution in the atmosphere (Sogalla et al., 2019; Katata et al., 2015). The comparison covers the time period from 40 hours to 75 hours after the accident initiation, which is when the major contributions to the FPs releases are believed to have come from unit 3.

Figure 4.8. **Unit 3 comparison of predicted cesium and iodine releases [Bq] versus backwards analyses (GRS and WSPEEDI)**

A. Cesium (Cs) B. Iodine (I)

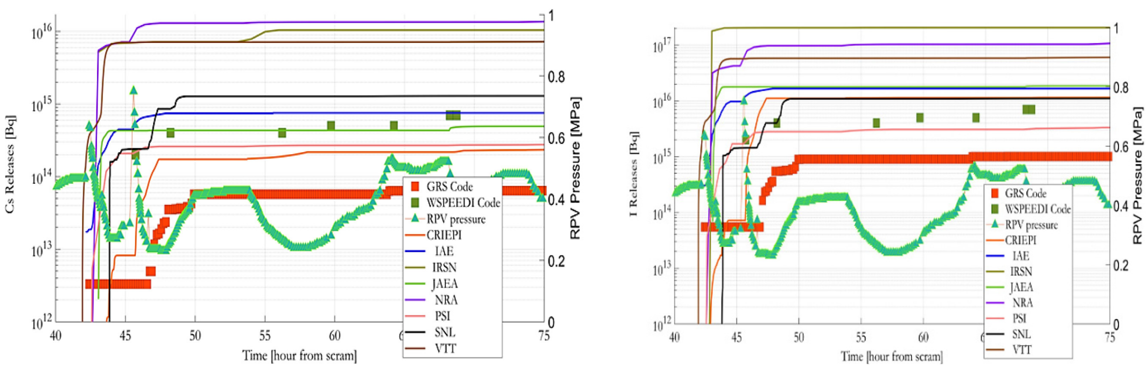

The comparison shows that the calculations with a large early release of Cs and I tend to significantly overpredict the integral release estimated by the GRS and WSPEEDI analyses. The rest of the calculations predicted a similar order of magnitude as the GRS and WSPEEDI analysis, indicating that the releases to the environment up until the hydrogen explosion should have been less than 0.5% of Cs and less than 2% of iodine. However, during the timeframe of the main release events in unit 3 (i.e. the first containment vents and the hydrogen explosion), the dominant wind direction was towards the ocean, thereby carrying the released FPs away from the land. This introduces additional uncertainty, as the releases calculated by the inverse methods during this time period rely on the activity measurements of samples of the ocean water.

Chapter 5. Atmospheric transport and dispersion: Results for Fukushima Daiichi units 1, 2 and 3

Many of the Benchmark Study of the Accident at the Fukushima Daiichi Nuclear Power Station (BSAF) Phase II participants provided source terms (STs) to be evaluated by Sandia National Laboratories (SNL)[1] by applying HYSPLIT (Draxler and Hess, 1998; Draxler, 1999; Air Resources Laboratory, 2016, 2017) to treat atmospheric transport and dispersion. The objective was to estimate the deposition pattern that would have resulted from the predicted ST. For the participants who provided results for all three units, the overall deposition pattern can be compared with the observed deposition pattern. For the participants who submitted STs for one or two units, the results can only be compared with each other. Atmospheric transport calculations were performed for a single isotope, Cs-137. It is the primary isotope of concern for long-term contamination and is relatively easy to measure due to the strong gamma signal produced from its short-lived decay product, Ba-137m. All of the atmospheric transport calculations used the actual location of each of the three units; the releases were not presumed to emanate from the same location. Also, when they were provided, release energies were accounted for in the analysis, so plume lofting was considered. Finally, aerosol size distribution data were considered for the purposes of estimating deposition. In some cases, aerosol size distribution can significantly influence deposition patterns.

Unit 1

Five of the organisations participating in Phase II of the BSAF (CIEMAT, the Institute of Applied Energy [IAE], the Radioprotection and Nuclear Safety Institute [IRSN], Korea Atomic Energy Research Institute [KAERI] and the SNL) submitted a unit 1 source term for atmospheric transport analysis. A comparison of these five source terms is shown in Figure 5.1. Of the five STs, three predicted a significant deposition over land (CIEMAT, KAERI and the SNL). The other two (the IAE and the IRSN) predicted nearly all the deposition over the ocean.

Unit 2

Six of the organisations participating in Phase II of the BSAF project (the Canadian Nuclear Laboratories (CNL), Central Research Institute of Electric Power Industry (CRIEPI), the IAE, the IRSN, KAERI and the SNL) submitted a unit 2 source term for atmospheric transport analysis. A comparison of these six source terms is shown in Figure 5.2. All except those from the IAE and the IRSN predicted significant deposition over land.

Unit 3

Six of the organisations participating in BSAF Phase II (CRIEPI, the IAE, the IRSN, KAERI, the Paul Scherrer Institute [PSI] and the SNL) submitted a unit 3 ST for atmospheric transport analysis. A comparison of these six source terms is shown in Figure 5.3. Three of the STs for unit 3 predicted significant deposition over land (the IRSN, KAERI and the SNL), while the other three (CRIEPI, the IAE and the PSI) predicted low-level deposition over land as well as over the ocean.

1. Sandia National Laboratories is a multi-mission laboratory managed and operated by National Technology & Engineering Solutions of Sandia, LLC, a wholly owned subsidiary of Honeywell International Inc., for the US Department of Energy's National Nuclear Security Administration under contract DE-NA0003525. SAND2018-8356 R.

Figure 5.1. **Unit 1 source terms for Cs-137 predicted by five BSAF participants**

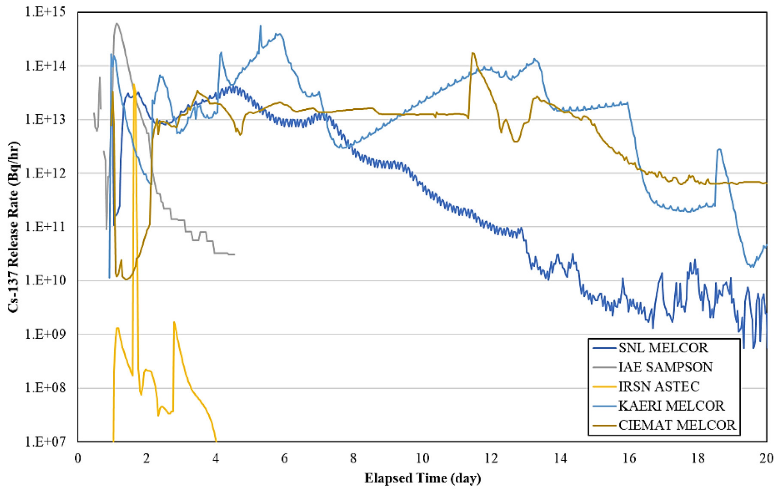

Figure 5.2. **Unit 2 source terms for Cs-137 predicted by six BSAF participants**

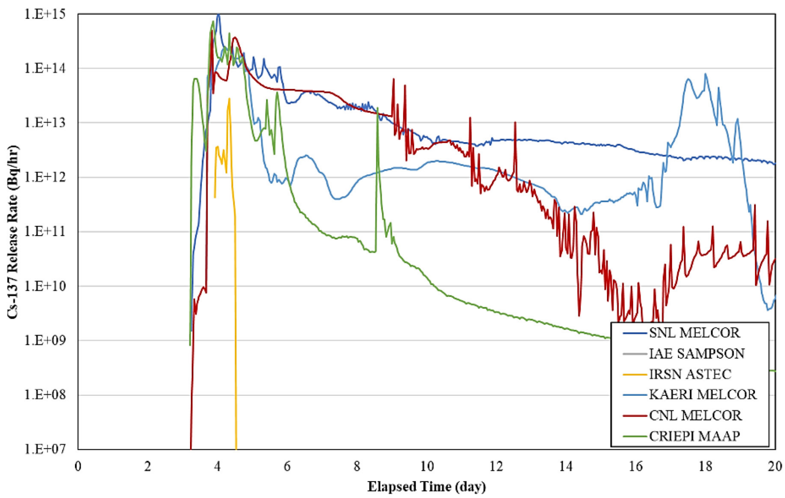

Figure 5.3. **Unit 3 source terms for Cs-137 predicted by six BSAF participants**

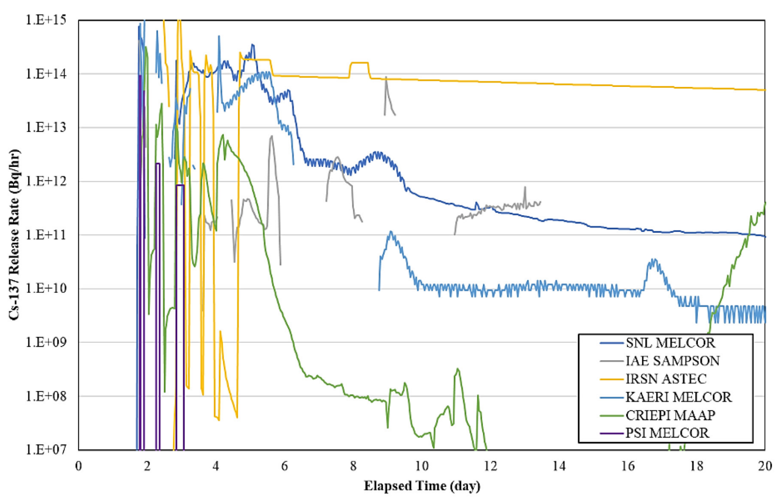

Comparisons for three units combined

Four of the organisations participating in Phase II of the BSAF (the IAE, the IRSN, KAERI and SNL) submitted a source term for all three units for atmospheric transport analysis. A comparison of these four STs is shown in Figure 5.4. Note that the land/ocean border is indicated by the light blue line that runs roughly north and south through the centre of the isopleth plots. The GRS used observational data from locations near the Fukushima site to reconstruct a source term. The observational data were interpreted using a newly developed method for the OECD BSAF Phase II project (see Chapter 6 of this report for a description of the method). As only land-based observations were available to the project, the ST calculated by the GRS has been augmented by published source term data based on the Japanese WSPEEDI model system for phases when radioactive releases are dispersed over the ocean. The deposition patterns predicted for the severe accident calculation STs are depicted in Figure 5.5, along with the calculated GRS source term (Figure 5.5e). For comparison, Figure 5.5f shows the measured Cs-137 isopleths using the same distance scale and using similar contour shading to facilitate the comparisons. However, note that the dark red contour level shown for the other results is not used there. The IAE source term predicted significant deposition over the ocean but very little over land, while the other three STs produced significant deposition over land. Each of these has unique characteristics, but all three have some features in common. These include: significant deposition (>3 MBq/m^2) out to 10-20 km towards the northwest; and a peninsula of deposition southward along the coastline. The deposition pattern for the GRS source term does not show the distinct peninsulas of deposition to the northwest or south along the seacoast that are observed in the severe accident calculations.

The Cs deposition to the northwest was observed, but such a high level of onshore deposition to the south was not. However, it has been noted that the sand along the seacoast to the south is heavily contaminated, which may indicate that significant deposition occurred slightly to the east (over the ocean) and resulted in contamination of the sand through wave and tidal interactions with the seashore (Katata et al., 2015). Thus, a peninsula of deposition to the south near the seashore is plausible.

Figure 5.4. **Combined three-unit source terms for Cs-137 predicted by five BSAF participants**

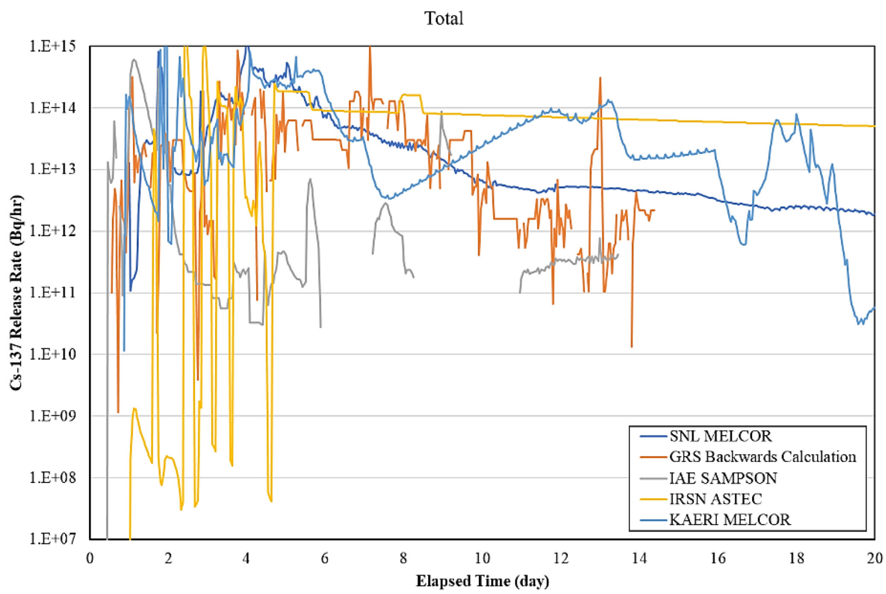

Figure 5.5. **Cs-137 isopleths for the three-unit source terms, the GRS/backwards calculation source term and observed ground deposition pattern for Cs-137**

A. IAE

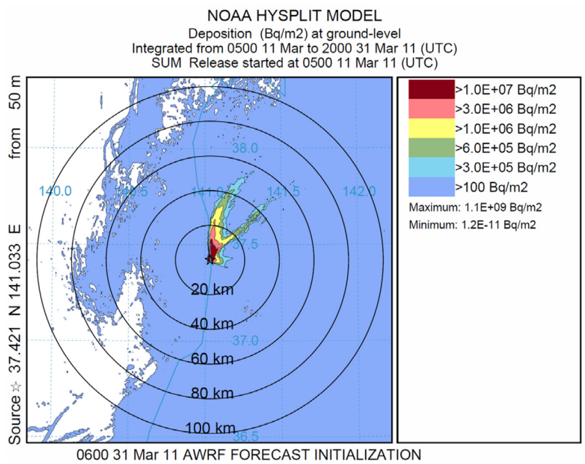

B. IRSN

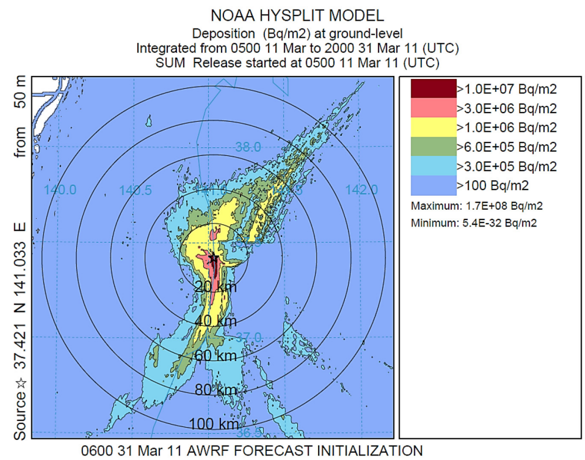

C. KAERI

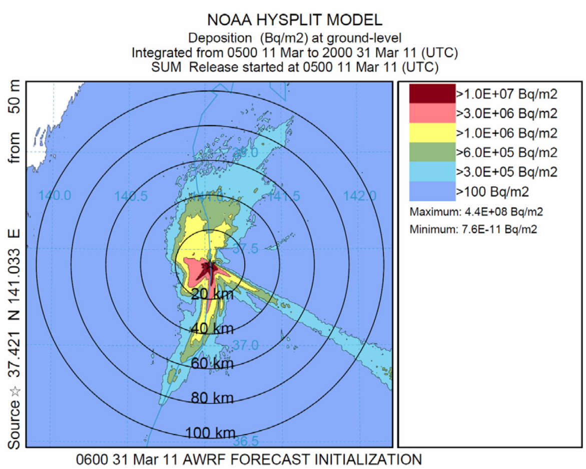

D. SNL

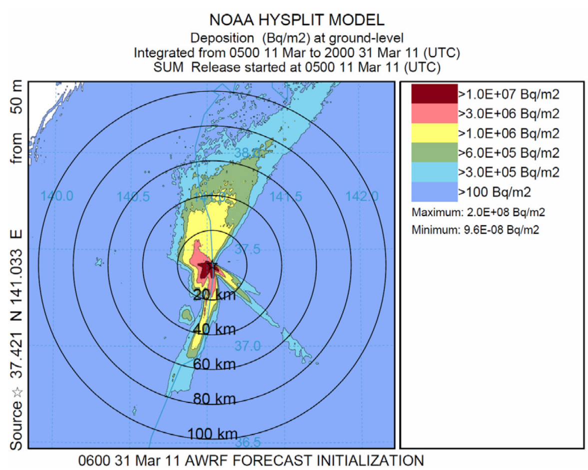

E. GRS/backwards calculation source term

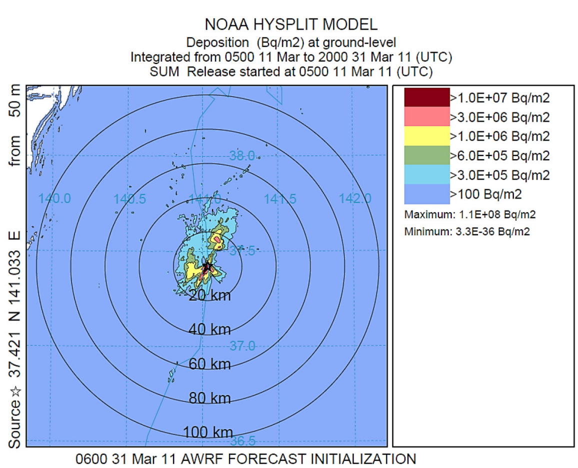

F. Observed ground deposition pattern for Cs-137

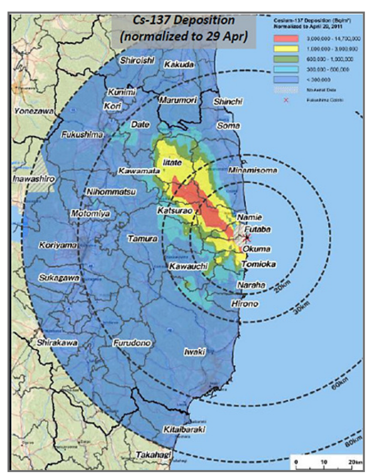

Estimated integral releases

Table 5.1 shows the integral releases of Cs-137 (in PBq) predicted by each of the BSAF contributors to this chapter and the combined releases for all three units for organisations that evaluated all the units. In the case of the GRS, individual units were not evaluated; instead, observational data were used to reconstruct a source term for the combination of the three units. In comparing these results to code analyses, the contribution of each unit was roughly estimated assuming that the release from the first failed unit (unit 1) stops when the release from the second failed unit starts (unit 3) and that this stops when the third unit (unit 2) fails.

Estimated releases from all three units range from 5.5 PBq to 43.2 PBq of Cs-137. Backwards calculation results are in the order of 13.1-14.5 PBq.

Table 5.1. **Integral releases of Cs-137 (PBq) predicted by BSAF participants**

	Code	Country	Unit 1	Unit 2	Unit 3	Combined
CIEMAT	MELCOR 2.1-4803	Spain	5.6			
CNL	MELCOR 2.1-6342	Canada		8.1		
CRIEPI	MAAP 5.01	Japan		6.7	0.8	
GRS	Backward calculation	Germany	0.79	10.7	1.6	13.1
IAE	SAMPSON-B 1.4 beta	Japan	4.4	0.0*	1.1	5.5
IRSN	ASTEC V2.0 rev3 p1	France	0.1	0.1	43.1	43.2
JAEA	WSPEEDI	Japan				14.5**
KAERI	MELCOR 1.8.6	Korea	18.9	5.8	10.9	35.5
NRC/DOE/SNL	MELCOR 2.1-5864	United States	2.8	12.3	10.6	25.7
PSI	MELCOR 2.1-4206	Switzerland			0.2	

* Little release predicted from the reactor building due to modelling deficit.

** See Katata et al., 2015.

Chapter 6. Radiological measurements and backward calculations of the source term

Dose rate measurements at the plant site and around

During the accident, the local dose rate was measured by the monitoring points (MPs) located at the plant site and around in the Fukushima prefecture (Figure 6.1). The available data are collected as Gy/h (or Sv/h). Since the measured value depends not only on the release time but also on the wind direction, meteorological conditions and deposition patterns, these data need to be analysed by atmospheric dispersion codes in order to confirm the actual release from the plant in Bq/h.

Examples of dose rate measurements performed by the Tokyo Electric Power Company (TEPCO) at some selected MPs are shown in Figure 6.2.

The beginning of the severe core degradation phases in units 1-3 is marked there as well. Those data have been made available through the Benchmark Study of the Accident at the Fukushima Daiichi Nuclear Power Station (BSAF) project, Phase II, and have been used for backwards calculation of the source term as discussed below.

Figure 6.1. **Monitoring posts within and around the Fukushima site**

A. Within the Fukushima site

B. Around the Fukushima site

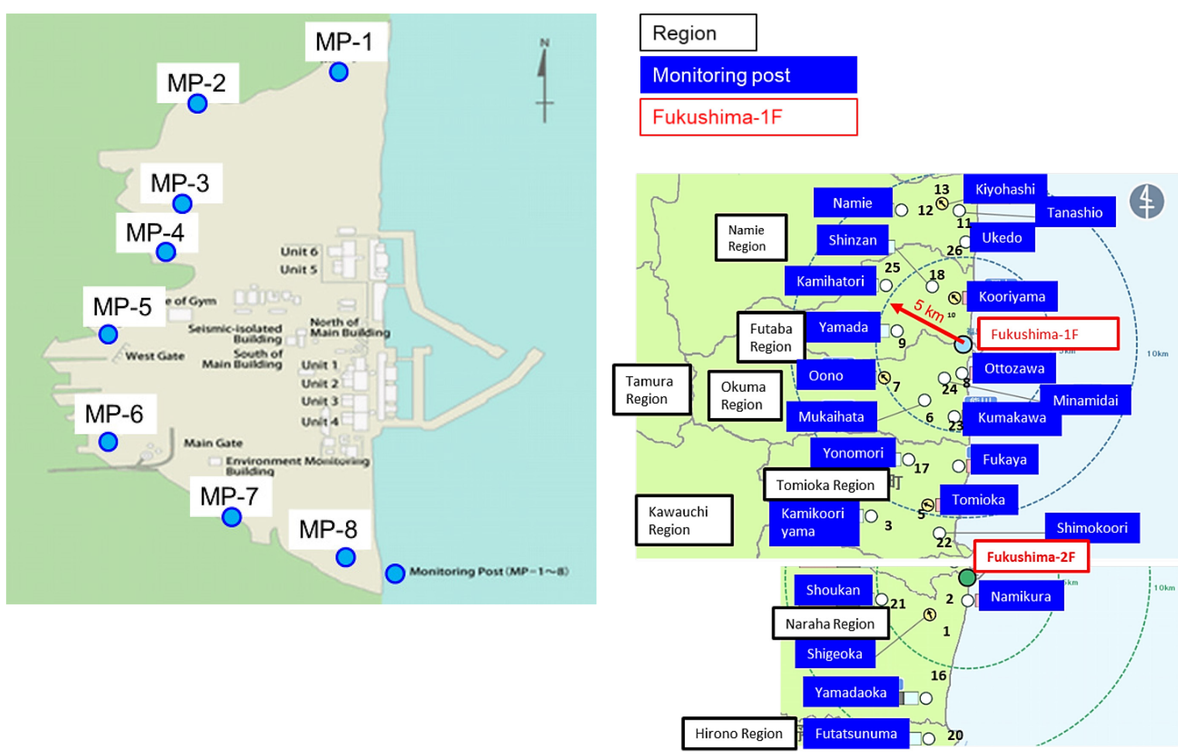

Figure 6.2. **Dose rate measurements performed by TEPCO at some selected monitoring points and start of severe core degradation phases in units 1-3**

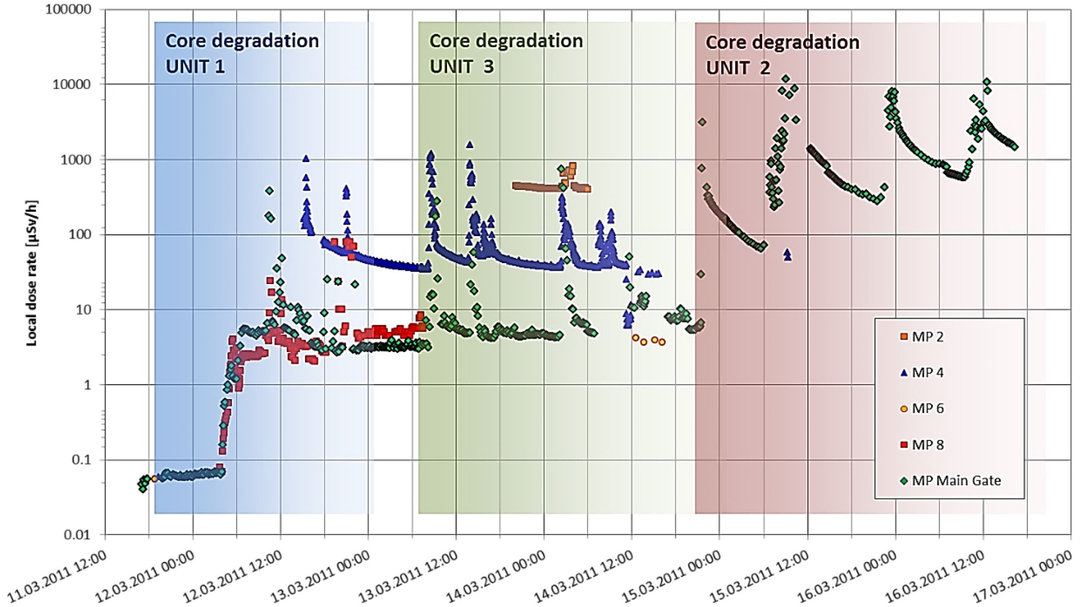

Dose rate measurements/samplings in the Pacific Ocean

Measurements of radionuclides by samples have been taken in the Pacific Ocean at various locations and time (Figure 6.3). Those measurements are relevant for several release periods of the accident, when the wind was blowing east towards the ocean. In these conditions, even though the radioactive plume was released by either venting or building leak, it would be undetectable by the MP or post measurements on land. The measurements of the ocean water samples were not available within the BSAF Phase II, but have been used in the source term (ST) estimation by the WSPEEDI code (Katata et al., 2015) described below.

Figure 6.3. **Sampling points in the Pacific Ocean**

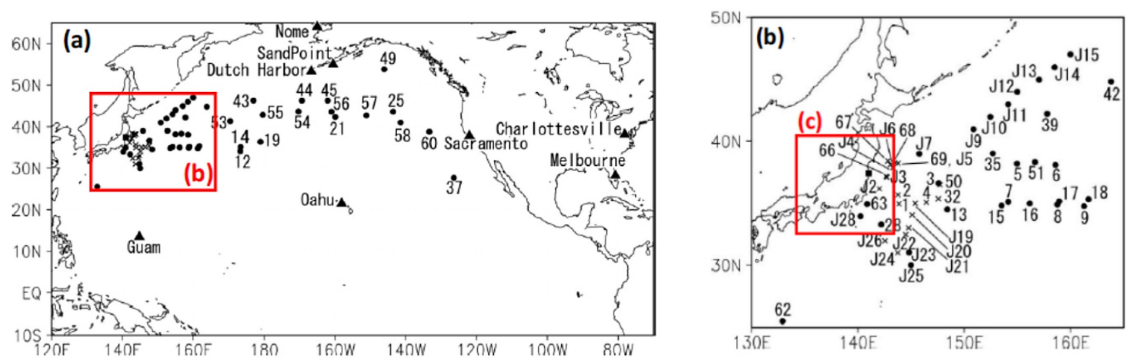

Source: Katata et al., 2015.

Backwards calculation of source term by WSPEEDI

The results of a detailed ST estimation based on the coupling of the WSPEEDI-II model to oceanic dispersion and sophisticated deposition models SEA-GEARN-FDM (Finite difference oceanic Dispersion Model) are described in Katata et al. (2015) (henceforth referenced as "WSPEEDI" for the sake of brevity). They relate observed features in the measured local dose rate to the activity release and selected available plant parameters during the accident progression. The investigation period covers more than the first month of the accident. The results have been used in Phase II of the BSAF for comparison against severe accident analyses.

The following brief sketch of the methodology for conducting the WSPEEDI analyses is provided as follows. Source term estimation was based on the reverse calculation of fission product (FP) releases which were related to radiological observations in the environment by atmospheric dispersion modelling. The preferred observational parameter measured over land for source term estimation was air activity concentration. When this parameter was not available, air dose rate measurements combined with samples of deposited nuclides were used. The distance of the accident site to radiological observations over land served as a basis for ST reconstruction and ranged from 4 km to over 80 km. The local dose rate measurements of the MPs at the Fukushima site (cf. MP-1-MP-8 in Figure 6.1a) were not included in the quantification of FP releases. During periods when released FP was mainly dispersed over the ocean, seawater concentration measurements in the Pacific Ocean at distances from a few hundred up to several thousand kilometres were used to correct land-based ST estimations (see Figure 6.3). For the distinction of different release phases, plant-based information and parameters were used. Active release phases were related to information on containment venting and hydrogen explosions in the buildings as well as on RPV and PCV pressure curves in units 1-3. Thus, the identification of active release phases was not independent from plant-related data assumptions. Between the distinct active release phases, a continuous release was assumed. The subdivision of these continuous release phases was mainly based on variations in the available radiological observations and was not linked to events in the plant. Within each release phase, the reverse calculation method applied yielded a constant release rate. If necessary, subjective corrections based on "expert judgement" (e.g. rotations of the modelled FP plumes) were applied to the modelled air concentration and dose rate fields to reduce discrepancies with the corresponding measurements.

The results of WSPEEDI source term calculations are summarised in Katata et al. (2015). Release rates until noon on 22 March 2011 are shown in Figure 6.4 as an example.

Figure 6.4. **Release rates from reactor scram on 11 March to 22 March 2011 computed by WSPEEDI**

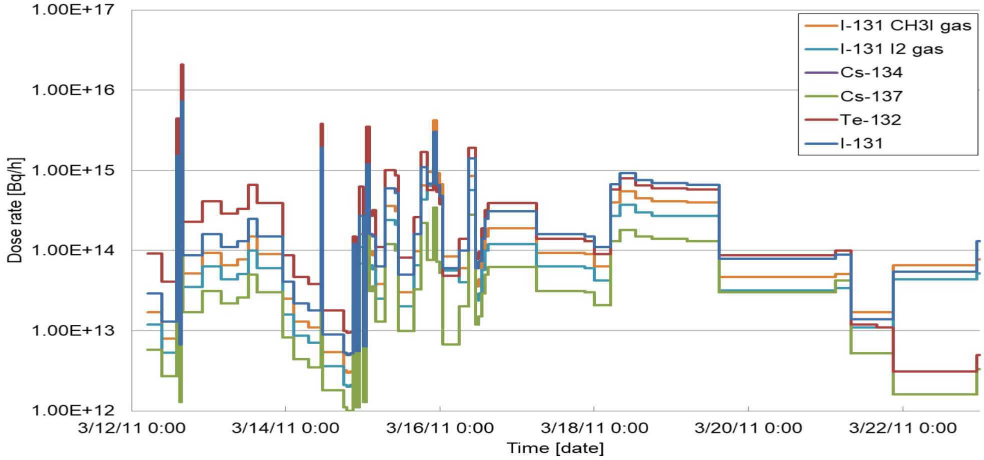

Source: Katata et al., 2015.

Backwards calculation of source term by the GRS method

Source term reconstruction at the GRS has been performed for the period from 12 March 2011 00:00 to 26 March 2011 00:00. The reconstruction method aimed at an optimised use of available radiological measurements at or nearby the Fukushima site (see Figure 6.1). It thus focused on the evaluation of the numerous local dose rate measurements on site or near the plant, while the nuclide composition had to be estimated from a limited number of available soil samples.

In contrast to the WSPEEDI analysis, a deliberately "blind" approach was followed, which omits the use of any plant information for identification/definition of release phases or quantification of releases. Measurement data of samplings from the Pacific Ocean at various locations and times, as presented in Figure 6.3, could not be used. The reconstruction scheme was based on the following steps.

Calculation of surface contamination from local dose rate and specific soil activity: For this step, measured local dose rates at each of the included MPs were divided into cloud shine caused by airborne radioactivity and ground shine caused by surface contamination. Then, nuclide-specific surface contamination was estimated by relating ground shine to the nuclide composition of the deposited nuclides, which in turn was determined from available samples of specific soil activity.

Calculation of air activity concentration from surface contamination and information on precipitation: Air activity concentration during cloud phases were calculated from the difference in surface contamination before and after the respective cloud phase. The respective deposition mechanism (dry or wet) was taken into account based on available information on precipitation. Deposition rates were assumed proportional to the strength of the cloud shine signal. This method yields estimates for the temporal development of air concentration of aerosols and elementary iodine, but not for possible contributions from noble gases.

Calculation of radioactive releases from local dose rate and air concentration and modelled dispersion: These calculations were performed with the Lagrangian dispersion model ARTM (Atmospheric Radionuclide Transport Model), which was developed by the GRS (Bundesamt für Strahlenschutz, 2018). Atmospheric transport dispersion parameters and gamma submersion factors were computed, which can be directly linked to calculated cloud shine at each MP. The quantity of radionuclides released was then calculated by an appropriate backward calculation method. For this purpose, an optimal solution for radioactive releases is sought by minimising the difference between the observed and calculated cloud shine that would result from the release estimate.

The database for ST reconstruction consists of local dose rate observations, soil activity concentration samples and meteorological measurements. The suitability of local dose rate measurements obtained at the MP depends on the integral length of observation, but also on the data coverage within the record. A suitable set of on-site MP at Fukushima Daiichi Nuclear Power Plant exists (see Figure 6.1a). The set of MPs for reconstruction was completed by local dose rate measurements in the surroundings, namely at the Fukushima Daini Nuclear Power Plant (MP-4) and MPs at Kiyohashi, Namie, Yamada, Oono, Yonomori, Shoukan and Yamadoaka (see Figure 6.1b). In addition, the MP at Kooriyama, Shinzan, Kamihatori, Minamidai, Mukaihata, Ottozawa, Shigeoka and Futatsunuma were employed for validation of the method.

Samples of specific soil activity are available at the Fukushima Daiichi Nuclear Power Plant from 21 March 2011. By the time of the first sample, possible releases of short-lived nuclides with half-lives of a few hours like I-132 would no longer be detectable in the deposits if they had occurred in the first few days of the accident. However, longer lived nuclides can be compared in the samples. For this purpose, all samples are decay-corrected to a common reference date (21 March at 00:00).

Based on this knowledge, I-132 was chosen as representative for short-lived nuclides which contributed to surface contamination. The amount of I-132 initially to be added to the basic nuclide composition to suitably explain observed local dose rates for each ground phase was calculated by a least square fit approach. This inclusion of I-132 in the nuclide vector especially enabled the proper consideration of the MPs at the site for ST reconstruction.

The computation of nuclide composition served as the basis for determining air concentration during cloud phases (Step 2) and performing the backward calculations (Step 3) for each MP. For Step 3, measurements of wind direction and velocity as well as precipitation information at the Fukushima Daiichi Nuclear Power Plant were used. Until the afternoon of 16 March 2011, additional weather data were available at the Oono MP, which were combined with measurements at the Fukushima Daiichi Nuclear Power Plant for use in the dispersion calculations.

Naturally, the observation of radioactive releases at each MP was confined to situations where the wind disperses the release approximately in the direction of the respective MP. Likewise, uncertainties in the quantification of the source term grow when the respective MP is only marginally affected by the dispersing radioactive cloud. These limitations and uncertainties can be reduced by the combination of backward calculation results for the ensemble of 14 above-mentioned MPs. For this purpose, the observed releases at each MP were weighted with the magnitude of dispersion parameters. The weighted average from each observation represents the common ST estimate based on this ensemble.

As observations over the ocean were not available for the BSAF project for our reconstruction, source term reconstruction was confined to time phases when releases were dispersed over land. Nevertheless, an observational coverage of about 50% was obtained for the first phase of the accident. During the occurrence of the largest measured peaks in local dose rate between the evening of 14 March 2011 and the afternoon of 16 March 2011 (Figure 6.2), observational coverage amounted to about 75%.

Reconstruction results are illustrated for the accumulated release of Cs-137 in Figure 6.5. It is evident that the weighted average provides a reasonable estimate of the Cs-137 release within the ensemble and that convergence between minimum and maximum estimates within the ensemble increases with time.

Figure 6.5. **Accumulated release of Cs-137 reconstructed by the GRS for the first two weeks of the accident**

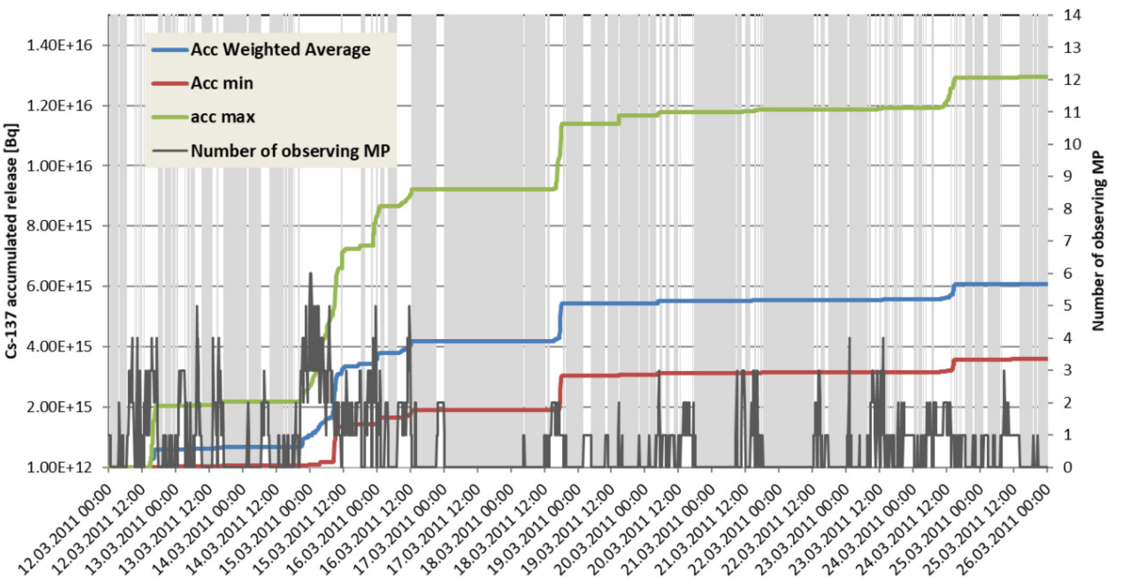

Note: Blue: weighted ensemble average; red: minimum estimate within ensemble of monitoring points; green: maximum estimate within ensemble; shaded: no observation by monitoring point ensemble possible; dark grey: number of observing monitoring points.

Comparison of the GRS and WSPEEDI source term calculation results

This section gives a comparison between the WSPEEDI source term estimation results and the GRS source term calculation results. The objective of this comparison is to take advantage of the higher temporal resolution and independent identification of active release phases of the GRS data set. By this, the validity of release phase subdivision within the WSPEEDI data set can be assessed and insights into possible links between active release phases and available information about accident progression can be broadened.

A clear advantage of the WSPEEDI method is the coverage of the whole investigation period, including those periods when the radioactive releases were dispersed over the ocean. On the other hand, through the participation in BSAF, the use of local dose rate measurements on the

Fukushima Daiichi Nuclear Power Plant site very close to the location of release was possible for the GRS. This enhanced the temporal resolution of the ST reconstruction and reduced the influence of errors and uncertainties on the dispersion calculations.

Figure 6.6 illustrates the calculated temporal development of radioactive releases obtained by both methods for Cs-137. For the sake of a clear visualisation, the GRS data were aggregated from a higher temporal resolution of ten minutes to hourly values. During most of the periods covered by both the GRS and WSPEEDI data (white background), the agreement between the curves is remarkably good, with some differences in the details of temporal development. During periods which were solely covered by WSPEEDI data (grey background), calculated release rates show mostly a uniform behaviour, with few variations. This lack of variation is presumably an effect caused by the lower temporal resolution achievable in these periods rather than by the release dynamics. This lower temporal distribution is caused by the reconstruction method, which relies on data based on samples from the ocean, which only provide aggregate deposition.

Figure 6.6. **Comparison of Cs-137 release rates obtained by the GRS (data aggregated to hourly values) and WSPEEDI source term reconstruction methods**

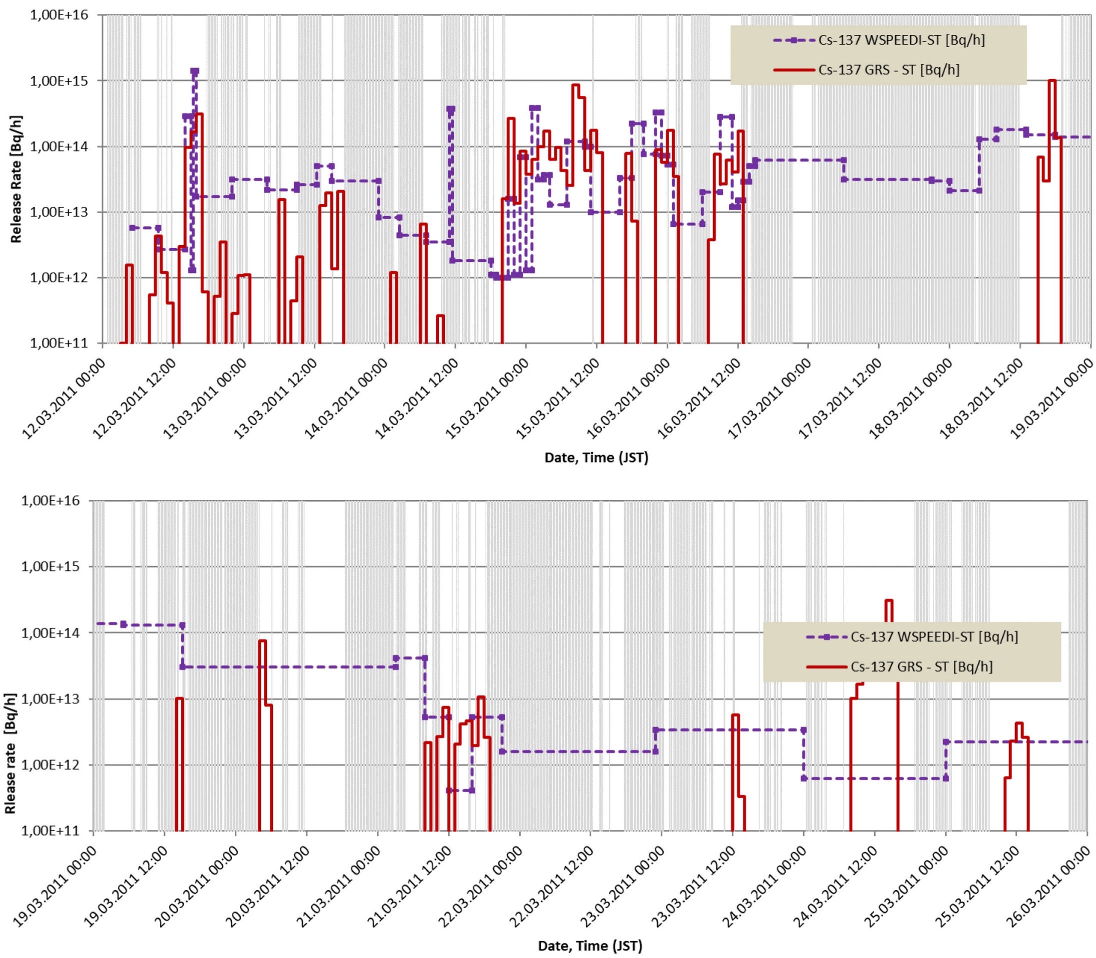

Note: Shaded: no observation by monitoring points ensemble used for the GRS backwards calculation possible.

The agreement between the results of the GRS and WSPEEDI calculations is pronounced in the comparison between accumulated releases of I-131 and Cs-137.

Figure 6.7. **Comparison of accumulated releases of Cs-137 and I-131 by the GRS and WSPEEDI source term reconstruction methods**

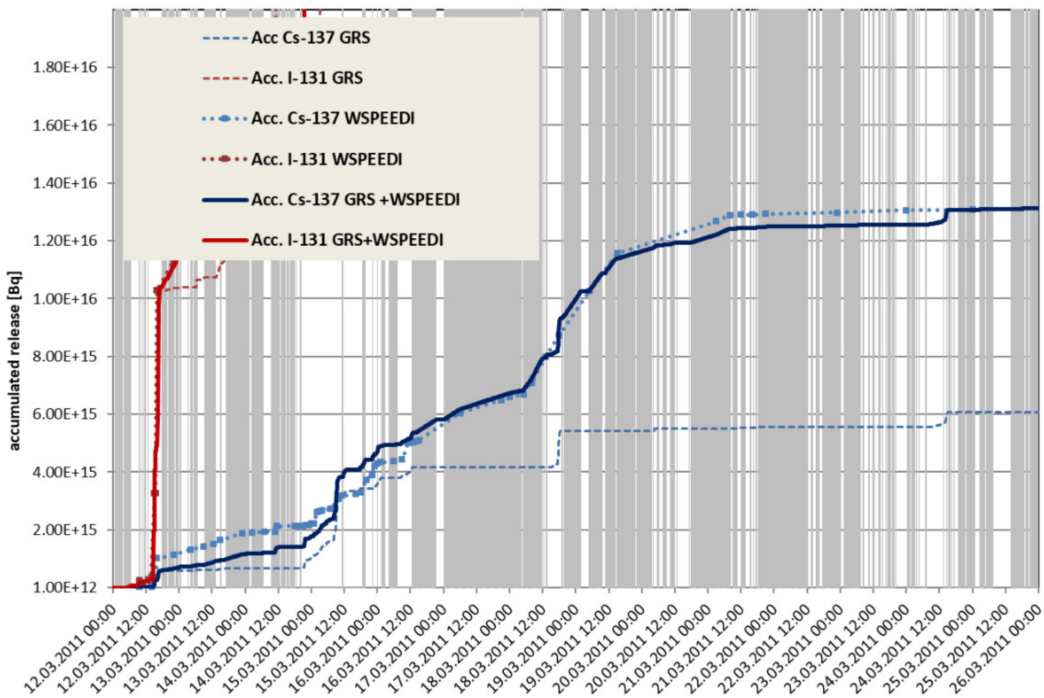

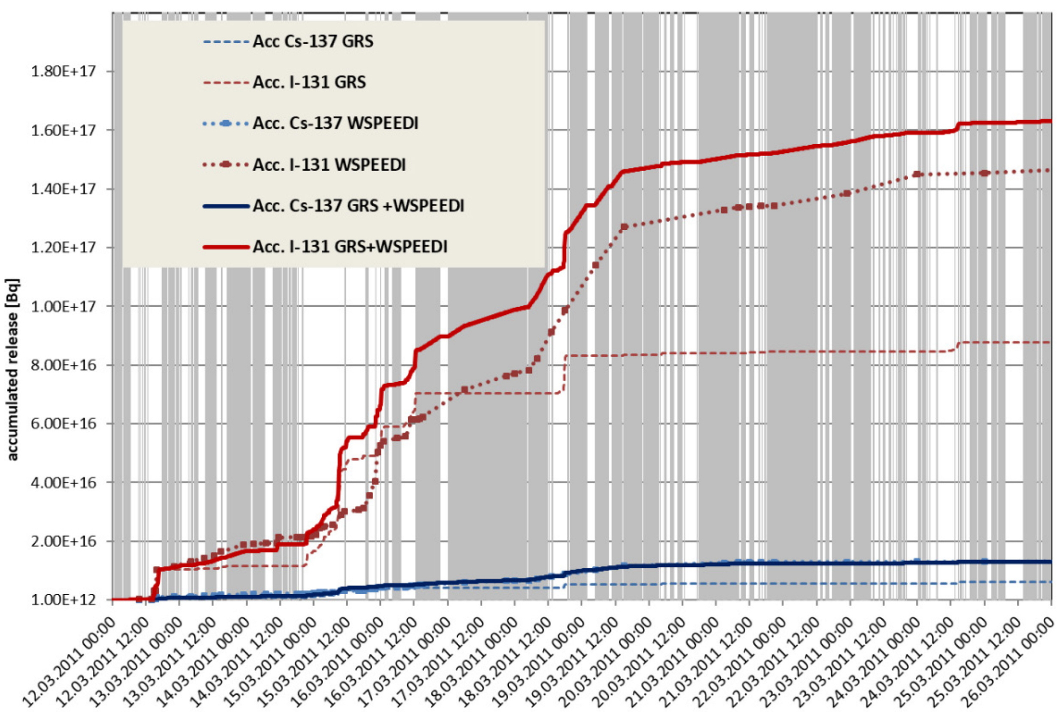

Notes: Blue: Cs-137; red: I-131; GRS (dashed); WSPEEDI (dash-dotted); shaded: no observation by monitoring point ensemble used for the GRS backwards calculation possible; solid lines: accumulated releases for combined GRS + WSPEEDI ST (GRS data gaps filled by WSPEEDI data).

Because of the striking agreement between the GRS and WSPEEDI source term results during periods covered by both methods, it seems reasonable to combine the ST results in the following manner. For periods covered by both the GRS and WSPEEDI results, the GRS data were taken as ST data because of their higher temporal resolution, larger number of nuclides considered and independent treatment of I-132. For periods not covered by the GRS data (wind direction towards the ocean), GRS data were completed by WSPEEDI data with respect to releases of I-131, Te-132, Cs-134 and Cs-137. This procedure combines the advantages of both data sets. The agreement between this combined "GRS-ST + WSPEEDI-ST" data set and the original WSPEEDI accumulated releases is nearly perfect, with maximum relative deviations of about 12% for iodine and less than 1% for cesium.

The results of this backwards calculation of the source term have been used for comparison of severe accident analyses results within the BSAF project and for an improved understanding of the accident progression. The calculated accumulated release amounts are nearly identical by the afternoon of 16 March 2011. Thereafter, the GRS calculation predicted lower integral releases than WSPEEDI, due to the increasing fraction of observational gaps in the GRS calculations, time periods where the wind was blowing towards the ocean. Nevertheless, after the first two weeks of the accident, the accumulated releases calculated by the GRS summed up to 60% of the WSPEEDI results for iodine and about 45% for Cs and tellurium (Te) isotopes. Differences in the calculated release amounts can thus be mainly attributed to the observational gaps in the GRS data.

Because of the striking agreement between the GRS and WSPEEDI source term results during the periods covered by both methods, it seems reasonable to combine the source term results in the following manner. For periods covered by both the GRS and WSPEEDI results, the GRS data were taken as source term data because of their higher temporal resolution, larger number of nuclides considered and independent treatment of I-132, whereas, for periods not covered by the GRS data (wind direction towards the ocean), the GRS data were completed by WSPEEDI data with respect to releases of I-131, Te-132, Cs-134 and Cs-137.

Chapter 7. **Lessons learnt and conclusions from the BSAF**

The current severe accident analyses have been carried out by various well-known severe accident codes and the results have been compared against major plant events and measurement data taken during the accident, such as the timing of the hydrogen explosions, reactor pressure vessel (RPV) water level, RPV pressure and primary containment vessel (PCV) pressure (suppression chamber and dry well). Phase II of the Benchmark Study of the Accident at the Fukushima Daiichi Nuclear Power Station (BSAF), thanks to the recent findings obtained during plant inspections (mainly muon and PCV internal assessment), allowed uncertainties regarding the current plant state to be drastically reduced. Comparisons with real evidence highlight some of the limitations of existing codes and identify areas that could benefit from novel experimental programmes and future code improvements.

Review of major technical findings

In the BSAF project, the severe accident analysis codes were used in two ways: 1) a forward approach, where the analysts allowed the code to predict the accident behaviour according to the current state of modelling; and 2) a forensic approach, where the analysts forced the code and/or boundary conditions to comply with observed events. Uncertainties in the measured data and observed events must be taken into account, too. During the calculations, the analysts may have needed to force certain events in their simulations in order to synchronise the predictions with the observed data. This might suggest that specific code models need refinement or improvement and validation, but it may also simply be a reflection of inherent natural and stochastic randomness and variability in the exact sequence and timing of key events in core degradation behaviour.

Core degradation: Major plant measurements, such as RPV and PCV pressure, or radiological measurements such as containment air measurement system (CAMS), may give indications of the occurrence of certain events, such as core relocation within the RPV, RPV failure, corium relocation from the RPV onto the cavity floor and containment failure.

This information can help to reduce uncertainties in predicting the timing and magnitude of key events. Uncertainties still exist regarding boundary conditions, such as the water injection during the reactor core isolation cooling (RCIC), high pressure coolant injection (HPCI) and external water addition, despite the development of new models that create more realistic representations. In addition, the state of the valves and rupture discs for containment venting system activations also remain a significant source of uncertainty. The magnitude of events such as pressure peaks are also uncertain. However, findings on how to adjust the simulation in order to reproduce the measurements can inform how core relocation models should be adjusted to better reflect the observations.

One typical source of scatter in the results of the calculations arises in the late stage of core degradation with the accumulation of debris on the core plate. In the boiling water reactor (BWR), this plate has a special design with many openings. It is uncertain if/how debris accumulates on the core plate or if the debris can independently relocate from each assembly to the lower plenum, either in between the control rod guide tubes or into it. This could affect the morphology of the debris in the lower plenum during the quenching period and affect the mode of lower head failure. Another possible method of corium relocation into the lower plenum is linked to molten pool formation, radial spreading of the molten pool above the core plate and ablation of the shroud wall; a scenario often assumed, especially in pressurised water reactors and heavily reflective of best understanding of the Three Mile Island 2 accident progression. This scenario represents additional uncertainty for the modelling of corium relocation from the core region.

The behaviour of control blades during the accident progression is also a major uncertainty. It is not known to what extent the boron carbide in the control blades was exposed to steam flow, producing volatile boric acid. The location and condition of residual peripheral structures in the units may provide some insight on the control rod behaviour.

In addition, modern severe accident (SA) analyses tend to predict early in-vessel melt progression as a slower process than previously thought two decades ago, driven largely by codes modelling more heat transfer pathways and accounting for more heat sink availability in the RPV and containment. In BWRs, the extensive upper internal structures in the RPV have the potential to melt and add steel to the core debris produced during accident progression. A major uncertainty related to this process is the heat transfer upward to these structures from the degrading BWR core. This also affects the heat transfer to gases from a degraded core configuration, which can contribute to possible failure of the main steam line due to creep; representing one of the existing uncertainties in the accident progression.

Core-concrete interaction: One striking result obtained in the BSAF activity is the extensive progression of the molten core concrete interaction (MCCI) predicted by all the codes (except dedicated MCCI codes such as TOLBIAC) for the unit 1 analyses and to some extent for unit 3, which continues without termination until 500 hours (the end of the simulation), independent of the water injection onto the debris. This continuous MCCI is inconsistent with internal inspection of the units, which show that the pedestal walls and structure are still mostly intact (i.e. the structure has not collapsed). Thus, the code predictions of the MCCI erosion seem to be overestimated and unrealistic, at least with respect to lateral erosion and pedestal wall attack.

Fission product release and transport: Regarding fission products (FPs), there are still several major uncertainties to be understood, including:

As suggested by the reverse FP analyses and some of the computer analyses, releases from damaged reactors likely persisted in between the readily observable transient burst releases associated with venting operations or containment failure/leakage events. Some codes (e.g. MELCOR) model revaporisation of volatile FP species such as CsI and Cs2MoO4 that are driven off of deposition surfaces by increasing structure temperatures, and other codes (e.g. Thales/Kirche) that consider ongoing evolution of gaseous iodine species such as I2 and CH3I, both of which lead to ongoing low level releases throughout the weeks following the accident.

While not generally modelled in the BSAF analyses, the transport of aqueous borne FPs that leak from the suppression pool or the PCV, or through the known underground water infiltration into and out of the reactor building lower compartments and turbine hall is known to exist, but not well characterised. Furthermore, leaching of FPs from submerged fuel debris into the PCV water pools is a persistent source term (ST) that can participate in the leakage of FPs from the PCV from water infiltration as well. These transport pathways could be better modelled in the SA codes if deemed important for predicting long-term FP releases. Finally, certain unusual FP forms have been observed, such as Cs silicate particles, where clear understanding of the origin of these forms is not clear and improvement in this area of ST characterisation may be useful.

User effects and uncertainty: It was also recognised during the project that a “user effect” is a major player in obtaining consistent results in the analysis of complicated transients. Variability in user-selected code input can lead to variability in the computed outputs, and likely reflect the uncertainty in predictive technologies in this area. Additionally, SA codes contain various points of occasional numerical instability that can contribute to excessive run-time code execution failures. The project has shown how scattering of the results from the various participants decreased from Phase I given the time for the analysts to become more and more experienced with BWR systems and modelling. The whole BSAF project also allowed participants to share experiences of multiple codes and consider how to improve models based on the maturity of other codes, thus strengthening the capabilities of all of the codes involved.

Fission product transport: Atmospheric transport and dispersion (ATD) of radionuclides from the Fukushima Daiichi site played a role in two different BSAF Phase II activities: 1) the estimation of deposition pattern that would have resulted from the predicted STs by the partners; and 2) the backwards calculation of the ST based on measured data such as local dose rates on-site or near the plant, samplings taken in the Pacific Ocean, and weather data. The phases when the wind was blowing either towards the Pacific Ocean or towards the land are known, and as such, the results of the calculated STs can be checked (e.g. the timing of the releases by the ATD calculations and the resulting overall deposition profiles). Larger uncertainties still have to be considered, as explained below.

Different weather data sets have been used by the Sandia National Laboratories (SNL) in the estimation of the deposition pattern based on source term data from the BSAF participants, providing significantly different results. The weather data set that seemed the most appropriate was selected. For the backwards calculation of the ST, other weather data sets were used by the GRS and the Japanese organisations using WSPEEDI. In conclusion, it is not entirely obvious which of the weather data sets best matches the observations.

Deposition patterns in the ATD analyses were only calculated for a single isotope, Cs-137, for the purposes of comparison to measurements of ground contamination by Cs-134 and Cs-137, while the backwards calculation provided results for other nuclides. Additionally, release energies associated with the source term data was accounted for in the analysis using the consideration of plume lofting. Finally, aerosol size distribution data were considered for the purpose of estimating deposition as, in some cases, aerosol size distribution can significantly influence deposition patterns.

It is well known that the results of both the deposition pattern and the backwards calculated STs were significantly influenced by the weather data set. Further analyses would therefore be needed to determine why the ST provided by the GRS backwards calculation, which is very similar to the Japanese WSPEEDI results, does not result in a similar deposition pattern as measured. It is recommended that future activities include a discussion and possibly a harmonisation of the weather data used, the deposition velocities for dry and wet deposition, and the simulated rainfall pattern in both activities. Furthermore, uncertainty bands linked to both activities should be determined. Nevertheless, these calculations provide important contributions to assess the calculated STs.

The results in Phase II can be considered to be much more robust than those in Phase I, as the understanding of the accident and its progression, and the experience and skills of the participants improved over the course of the project, and additionally, many plant inspection results have since been provided by the Tokyo Electric Power Company (TEPCO).

The first advancement from the Phase I efforts regards the information about the plant internals and current status of the units. Muon inspections of the RPVs and robot inspection of the PCVs yielded significant information in order to discern between realistic and not realistic scenarios. The muon imaging investigation showed that very little debris still exists in the core region of all the units. It also showed very little debris in the lower head of unit 1, while some high-density debris was identified in units 2 and 3. The PCV internal investigations in all the units revealed ex-vessel debris in all the units. For units 2 and 3, whose status was uncertain in Phase I, the ex-vessel nature of the accidents became obvious through the camera inspections of the PCV, which showed evidence of debris through the videos.

The second advance from Phase I was the identification of the critical parts of the accidents that, thanks to TEPCO's support, were stressed throughout the project. In particular, the focus on the period of core degradation (e.g. three peak periods for unit 2, or the time before the modelled automatic depressurisation system (ADS) activation in unit 3). This approach stimulated the participants to make a particular effort in specific parts of the transient, which were considered critical for the explanation of the accident and identification of debris distribution.

Finally, it needs to be recognised that the understanding of the nature of a severe accident evolved throughout the project. Historically, the most studied example of a severe accident is the Three Mile Island 2 accident. However, this accident was very different from the Fukushima accidents and the pressurised water reactor (PWR) reactor design involved in Three Mile Island 2 is quite different from the Fukushima Daiichi BWRs, which also included a different accident for each of the three units. Therefore, participants required time to become familiar with the Fukushima Daiichi design in particular, because it involved very detailed knowledge of the plant, which had generally not been addressed in previous studies (e.g. difference between control rod and control rod guide tube, structures below the lower plenum, details of RCIC/HPCI, details of valves, etc.).

Review of major impacts to the BSAF stakeholders

Research programmes such as the BSAF1 and BSAF2 projects, because of the large stakeholder group size, have the potential to produce impact on the nuclear community at large. Some of the important impacts of the BSAF studies on the diverse stakeholders are summarised below. Stakeholders include the international research community of scientists and engineers, government and regulatory bodies, industry partners including TEPCO, and the general public.

First, for code developers and accident analysts, the BSAF efforts provided a unique opportunity to apply codes to real-world accident conditions. In the process, the BSAF projects have resulted in the development of a skilled collective of human knowledge that is now moving to apply the knowledge gained from BSAF improved code models for melt progression and more confident application of severe accident codes to both existing plants and emerging next-generation plants. This collective will also be extremely useful to the future Fukushima-related OECD efforts, as well as ongoing activities related to Fukushima site decommissioning. A review of some of these accomplishments, gained knowledge and areas for code model improvements follows.

Impact on code developers and severe accident analysts: The BSAF analytical efforts have led to greater confidence in the predicted accident progression as well as awareness of the inherent variability and uncertainty in the code results. It also emphasised the inherent differences between BWR core melt progression and those in PWRs. The close integration of TEPCO insights and emerging information about the state of each reactor has allowed identification of potential code and model improvements in a number of complex areas, such as suppression pool thermal stratification, material interactions (especially zirconium interactions with fuel and RPV structures), the mode of vessel head failure and release of core materials to the cavity region, and the degree of core debris attack on the cavity concrete. These are a few of the focus areas that will be addressed by code developers and analysts in ongoing investigations of the Fukushima accidents.

Impact on regulatory practice: The BSAF project has contributed to a good understanding of the detailed progression of each of the Fukushima accidents and has thereby improved regulatory confidence of oversight of severe accidents, containment performance and their potential source terms to the environment. This additionally improves public confidence in that regulatory oversight. Increased regulatory competency in severe accidents will help ensure that regulations are as effective as possible and that adequate safety margins exist in the current regulations. Regulatory considerations of severe accident issues have been improved by the BSAF with respect to understanding what happened in the accidents, and regulator/public confidence in nuclear technology and its regulation for safe societal use have also improved. Industry has also been strongly affected by the project's results through improved understanding of what happened in the accidents and by extension, how accidents can be better managed. Some of the industry impacts of the project are discussed below.

Impact on industry practice in severe accidents

- Severe accident management and guidelines (SAMGs) – The Electric Power Research Institute (EPRI) and the BWR and PWR Owners groups have followed the BSAF programme and applied the lessons learnt to the refinement and improvement of both the severe accident guidelines recommended by the community and the education and competency of the utility industry in the phenomena and impacts of severe accidents on power plants.
- Vessel breach signatures used in navigating the SAMGs are likely problematic in that significant fractions of debris are likely to remain in the vessel even after initial failure of the lower head.
- Severe Accident Water Addition (SAWA)/Severe Accident Water Management (SAWM) is a recent SAMG development arising from the understanding of the Fukushima containment performance and improved containment protection by water addition (SAWA) and in the optimum use or "management" of water (SAWM) in US BWRs. Real-world evidence from Fukushima and the BSAF efforts have provided the technical basis for these accident management procedures.

- With fuel debris likely clumping in the reactor pedestal initially on steel structures below the vessel, the impact on a dry well-only injection point requires further evaluation to understand the extent to which cooling will reach the ex-vessel debris bed.
- Containment protection and venting: Thinking is evolving regarding the potential for containment protection from the over-pressurisation seen in the Fukushima accidents, where early venting before significant accumulation of fission products in the PCV can be a strategy to prevent radioactive releases later as containment challenges become severe.
- Liner melt-through appears to be a less likely outcome, at least in the timeframe following lower head failure, based on the analytical findings of many BSAF analyses of the Fukushima accidents.
- Risk-informing flex equipment requirements in the long run (long-term maintenance cost): This is greatly facilitated by increased confidence in the application of severe accident codes that have successfully captured the essential signatures of the Fukushima accidents.

A special case of industry impacts can be identified for both TEPCO as well as the Japanese organisations tasked with decommissioning the Fukushima site. Some additional impacts for Japanese industry follow.

Impact on Fukushima site decommissioning and Japanese industry stakeholders

Collaboration between TEPCO and the BSAF programme has significantly improved TEPCO's and the Japanese nuclear industry's understanding of the accidents and, in time, will improve public confidence in nuclear plant safe operations across their fleet. The confidence gained in code analysis of these complex accidents also will allow the codes to be used to inform decommissioning activities where predicted damaged fuel distribution within the RPV and PCV allow for comprehensive assessment of potential points of entry into the PCV to remove fuel debris, and estimates of material composition of relocated fuel debris allow evaluation of potential material cutting requirements through the testing of unirradiated material surrogates informed by analysis. Finally, the decommissioning activities will no doubt reveal other phenomena of potential significance to code modelling capability. Further scientific understanding and code improvements can be realised by examining and characterising materials recovered from the damaged reactors – the BSAF foundations provide an informed basis for efficiently and with minimal additional costs identifying areas where scientific understanding can be advanced through inspections and sample analyses obtained during decommissioning.

These aspects of BSAF support for decommissioning activities have been one of the programme's focuses from the onset, and the body of knowledge and technical competency will greatly improve TEPCO's success in decommissioning activities that will be ongoing for decades. Next, we turn to the impacts on public perception.

Impact on public confidence in the nuclear industry

Public confidence regarding the nuclear industry is understandably tenuous, and accidents such as Three Mile Island 2, Chernobyl and Fukushima present powerful reminders that nuclear technology must be handled with care and the highest levels of safety. As the existential threats posed by climate change and global warming put increased pressure on traditional carbon-based energy sources, it is ever more critical that the nuclear industry demonstrates understanding and competency in the use of nuclear technology for low-carbon energy in the future. The BSAF effort contributes to this by advancing public knowledge and confidence and dispelling unwarranted fears. This is a worthy ambition.

Overall conclusions

The BSAF project has been the most significant assessment of severe accident code capabilities to date against real-world accidents, providing a benchmark of several major integral severe accident analysis codes. In a way similar to the other benchmark study, Phase I was conducted as a sort of blind test due to lack of the accident progression information and end state of the

Fukushima Daiichi accident plant. At the same time as Phase II started, considerable information inside the RPV and PCV was obtained through direct and indirect investigation. Therefore, Phase II of the project was conducted with well-organised information provided by the operating agent with support from the Tokyo Electric Power Company (TEPCO). After two phases and six years of continued analysis, the BSAF project has led to a significant increase in the state of knowledge of the progression and associated consequences for boiling water reactor (BWR) severe accidents. As information has become available through forensic evaluations and engineering analysis, the state of the art of severe accident modelling practices has been significantly improved. This can be seen in the development of new phenomenological models and code performance enhancements, which enabled Phase II participants to model a full three weeks following the initiation of the accident, a feat not possible at the beginning of the project. The project has established a firm basis for future analysis and has also highlighted key phenomenological gaps in our understanding of severe accidents. These include component (e.g. reactor core isolation cooling – RCIC) behaviour, core damage progression in Zr/SS-rich debris (BWR specific), lower head attack and failure mode, persistence and aggressiveness of the molten core concrete interaction (MCCI), and radionuclide revolatilisation. The participating organisations look forward to continuing these activities in the coming years and projects.

References

Air Resources Laboratory (2017), "Weather data archive", National Oceanic and Atmospheric Administration, Silver Spring, MD, ftp://arlftp.arlhq.noaa.gov/archives.

Air Resources Laboratory (2016), "HYSPLIT user's guide", National Oceanic and Atmospheric Administration, Silver Spring, MD, www.arl.noaa.gov/documents/reports/hysplit_user_guide.pdf.

Bundesamt für Strahlenschutz (2018), "Atmospheric Radionuclide Transport Model (ARTM) and its dose module (DARTM)", Federal Office for Radiation Protection, Salzgitter, Germany, www.bfs.de/EN/topics/ion/environment/air-soil/emission-monitoring/artm.html.

Draxler, R.R. (1999), "HYSPLIT4 user's guide", NOAA Technical Memorandum ERL ARL-230, National Oceanic and Atmospheric Administration, Silver Spring, MD, www.arl.noaa.gov/wp_arl/wp-content/uploads/documents/reports/arl-230.pdf.

Draxler, R.R. and G.D. Hess (1998), "An overview of the HYSPLIT_4 modeling system of trajectories, dispersion, and deposition", *Australian Meteorological Magazine*, Vol. 47/4, pp. 295-308, www.arl.noaa.gov/documents/reports/MetMag.pdf.

Katata, G. et al. (2015), "Detailed source term estimation of the atmospheric release for the Fukushima Daiichi Nuclear Power Station accident by coupling simulations of an atmospheric dispersion model with an improved deposition scheme and oceanic dispersion model", *Atmospheric Chemistry and Physics*, Vol. 15/2, pp. 1029-1070, https://doi.org/10.5194/acp-15-1029-2015.

Richter, C., H. Thielen and M. Sogalla (2015), *Ergänzende Untersuchungen zur Validierung des Atmosphärischen Radionuklid-Transport-Modells (ARTM)*, GRS-394, GRS, www.grs.de/sites/default/files/pdf/grs-394.pdf.

Sogalla, M. et al. (2019), "Reconstruction of the Fukushima source term from nearby radiological measurements", paper provided for NURETH-18, Portland, OR.

TEPCO (2017a), "Evaluation of the situation of cores and containment vessels of Fukushima Daiichi Nuclear Power Station units 1 to 3 and examination into unsolved issues in the accident progression", Progress Report No. 5, Attachment 3-8, "Leaks from the Unit-3 PCV and steam release in a large amount", Tokyo Electric Power Company, www.tepco.co.jp/en/press/corp-com/release/betu17_e/images/171225e0240.pdf.

TEPCO (2017b), "Locating fuel debris inside the Unit 3 reactor using a muon measurement technology at Fukushima Daiichi Nuclear Power Station", Tokyo Electric Power Company, www.tepco.co.jp/en/nu/fukushima-np/handouts/2017/images/handouts_170928_01-e.pdf.

TEPCO (2014), "Results of water level measuring inside the suppression chamber (S/C) at the Unit 2 in Fukushima Daiichi NPS", Tokyo Electric Power Company, www.tepco.co.jp/en/nu/fukushima-np/handouts/2014/images/handouts_140121_04-e.pdf.

TEPCO (2013), "Results of investigation around lower parts of Unit 1 vent pipes at Fukushima Daiichi NPS (second day)", Tokyo Electric Power Company, www.tepco.co.jp/en/nu/fukushima-np/handouts/2013/images/handouts_131114_05-e.pdf.

Uchida, S. et al. (2021), "An approach toward evaluation of long-term fission product distributions in the Fukushima Daiichi Nuclear Power Plant after the severe accident", *Nuclear Engineering and Design*, Elsevier, https://doi.org/10.1016/j.nucengdes.2021.111256.

NEA PUBLICATIONS AND INFORMATION

The full catalogue of publications is available online at www.oecd-nea.org/pub.

In addition to basic information on the Agency and its work programme, the NEA website offers free downloads of hundreds of technical and policy-oriented reports. The professional journal of the Agency, *NEA News* – featuring articles on the latest nuclear energy issues – is available online at www.oecd-nea.org/nea-news.

An NEA monthly electronic bulletin is distributed free of charge to subscribers, providing updates of new results, events and publications. Sign up at www.oecdnea.org/bulletin.

Visit us on LinkedIn at www.linkedin.com/company/oecd-nuclear-energy-agency or follow us on Twitter @OECD_NEA.

OECD/NEA PUBLISHING, 2 rue André-Pascal, 75775 PARIS CEDEX 16

Benchmark Study of the Accident at the Fukushima Daiichi Nuclear Power Plant

Understanding the accident at the Fukushima Daiichi Nuclear Power Plant is important for safe and timely decommissioning of the reactors. This objective, together with the development of better computer codes for analysis of severe accidents, was the aim of the benchmark study conducted under the auspices of the OECD Nuclear Energy Agency. Through the diversity of the modelling codes and approaches, and the use of parametric studies, it has been possible to identify the more likely scenarios that can fit with the limited data available from the accident. The insights gained from the project will help guide research into severe accident behaviour, improve severe accident computer codes, develop accident mitigation and response at nuclear power plants, support regulatory oversight related to severe accidents, and inform policies on the development and deployment of nuclear technology.

Nuclear Energy Agency (NEA)
46, quai Alphonse Le Gallo
92100 Boulogne-Billancourt, France
Tel.: +33 (0)1 73 21 28 19
nea@oecd-nea.org www.oecd-nea.org

NEA No. 7525